Synthesis, Characterization of Nanocellulose and Surface-modified Nanocellulose for Various Pharmaceutical Applications

SUMMARY FOR THE DEGREE OF

DOCTORATE OF PHILOSOPHY (Ph.D.)

In

Pharmaceutical sciences

By

Miss Shweta Mishra

Under the guidance of

Dr. Bala Prabhakar

Shobhaben Pratapbhai Patel

School of Pharmacy & Technology Management

SVKM's NMIMS

Mumbai-400056

2023

1 INTRODUCTION

Biopolymers have intrigued humankind since the dawn of civilization. Polysaccharides are the most abundant of the three major types of biopolymers. Cellulose is the most common biopolymer on Earth, with annual production above 75 billion tonnes [1]. The 'PubMed' search using the term 'Cellulose' yielded 104154 hits (conducted on December 21, 2022). This many hits only emphasize the utility of cellulose and its derivatives. Countless research and review articles have been published describing the utility of cellulose-based materials in electronics [2][3][4][5][6], bioethanol production [7][8][9] specialty chemicals production [10][11][12] biomedical and allied fields [13][14][15][16][17] and many others. In recent years, cellulose and its derivatives have attracted significant attention, primarily due to a) increased awareness of the availability of its resources, mainly from agricultural waste or biomass [18][19],b) improved methods of their production [20][21][22][23] and c) recent developments in the techniques for cellulose solubilization and selective chemical modifications [24][25][26].

Lignocellulosic biomass is mainly within the plant cell wall, which composes of structural carbohydrates of homogeneous cellulose (35–50%), heterogeneous hemicelluloses (20–35%), as well as phenolic polymer lignin (10–25%) as primary components. The remaining fraction of lignocellulosic biomass includes proteins, oils, and ash.

There are regions of these cellulose fibrils where the cellulose chains are grouped in a highly ordered (crystalline) form, and there are others where they are disordered (like amorphous materials). There is still confusion about the organization and distribution of these crystalline and amorphous domains inside cellulose fibrils. However, to produce cellulose nanocrystals (NCCs), these crystalline regions found within the cellulose microfibrils are extracted.

Cellulose is a polysaccharide composed of linear glucan chains linked together by β-1,4-glycosidic bonds with cellobiose residues as the repeating unit at different degrees of polymerization (DP) and packed into microfibrils which are held together by intramolecular hydrogen bonds as well as intermolecular van der waal forces. These cellulose fibrils serve as the primary phase of reinforcement for bacteria, algae, certain marine organisms (such as tunicates), trees, plants, and some types of algae. Certain bacteria release cellulose fibrils, which help to form an exterior network structure [27].

Crystalline cellulose exists in several types of polymorphs (I, II, III, and IV). Cellulose I is

crystalline cellulose that is naturally produced by a variety of organisms (trees, plants, tunicates, algae, and bacteria). It is also known as natural cellulose. Cellulose I is thermodynamically metastable and can be converted to polymorphs II or III. The most stable cellulose polymorphs among all are type II and they can be produced by two processes: regeneration (solubilization and recrystallization) and mercerization (aqueous sodium hydroxide treatments). Cellulose II has monoclinic structure and is used to prepare transparent films [28].

Cellulose I or II may be converted to Cellulose II by using liquid ammonia treatment, and Cellulose IV can subsequently be formed using additional heat treatments. Cellulose I exist in two polymorphs, a triclinic structure (I_a) and a monoclinic structure (I_b). These polymorphs coexist in different proportions depending on the different sources. I_a cellulose polymorph is mostly found in algae and bacteria whereas I_b is usually found in plant cell wall and tunicates. I_a can be converted into the I_b by hydrothermal treatments in alkaline solution and high temperature reaction in organic solvents with helium gas. However, complete conversion to I_b is typically not achieved.

Cellulose chains are organized in a pattern known as "parallel up" in both I_a and I_b unit cells. The 1-to-4 linkage (1-4 linkage) throughout the length of the cellulose chain alters how nearby chains interact with one another because the cellulose repeat unit has a distinct structure on each side of the 1-4 linkage. When all the cellulose chains are arranged in 1–4 in the same direction, the word "parallel" is used. Contrarily, "antiparallel" refers to the alternate stacking of cellulose chains in the directionality of 1 to 4 links between various hydrogen bonding planes.

Although polymorph has been documented for cellulose, X-ray diffraction analysis indicates that native cellulose occurs as cellulose I, a mixture of polymorph I_α and I_β. Cellulose I_α is synthesized simultaneously with the extension of the microfibril network, which is dominant in some bacteria and lower plants to form the primary wall, but cellulose I_β is deposited mainly within the secondary wall of higher plants for strength. The decipherment of crystalline structure for cellulose indicates that cellulose I_α is characterized by the triclinic unit containing one chain, while there are two chains in the monoclinic unit of cellulose I_β for more intramolecular hydrogen bonds, making it more stable.

2 AIM & SCOPE

2.1 RATIONALE

Nanocrystalline cellulose is an emerging sustainable biomaterial with exceptional physicochemical properties. Current methods of producing NCC use wood pulp or cotton linters. Wood cellulose is the most extensively used biomass for isolating nanocellulose. Alternate sources and cost-efficient methods of production of NCC have to be explored. It can be isolated from inexpensive renewable cellulosic biomass.

To our knowledge, no one has explored banana peels and sugarcane derived microcrystalline cellulose for extraction of NCC. Such a renewable source for NCC production will also save thousands of trees from cutting. With much chemical functionality within the NCC structure, these building blocks provide a unique platform for significant surface modification through various methods. The modified NCC can be explored for various pharmaceutical applications such as superdisintegrant and solubility enhancer.

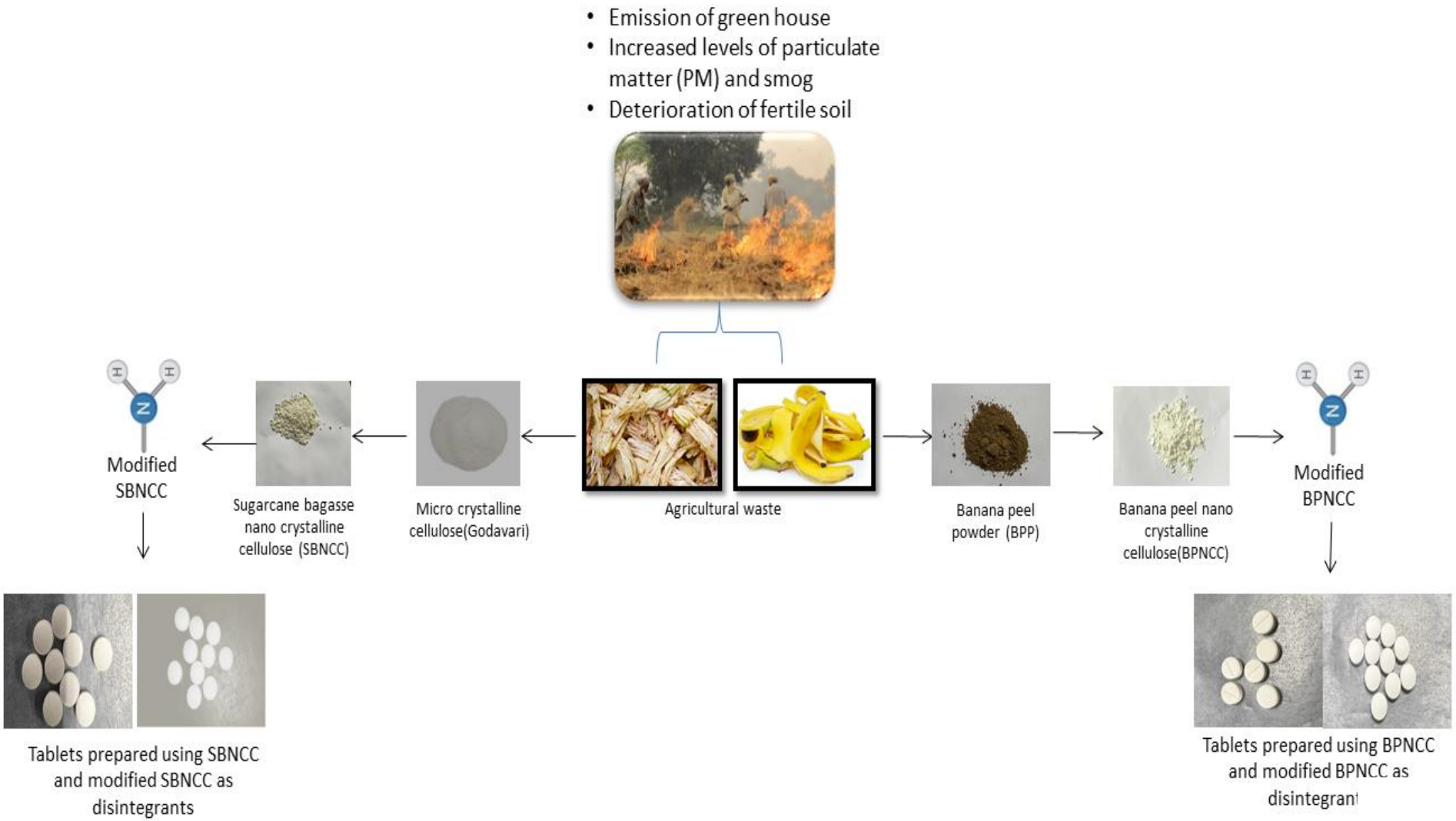
• Emission of green house
• Increased levels of particulate matter (PM) and smog
• Deterioration of fertile soil
Agricultural waste
Micro crystalline cellulose(Godavari)
Sugarcane bagasse nano crystalline cellulose (SBNCC)
Modified SBNCC
Tablets prepared using SBNCC and modified SBNCC as disintegrants
Banana peel powder (BPP)
Banana peel nano crystalline cellulose(BPNCC)
Modified BPNCC
Tablets prepared using BPNCC and modified BPNCC as disintegrant

Figure 1 Graphical abstract of proposed work

2.2 OBJECTIVES

The specific objectives of the research work are -

- Synthesis and characterization of NCC from various sources (Agricultural waste and sugarcane derived bagasse MCC)
- Synthesis and characterization of various derivatives of NCC
- To test the applicability of NCC and modified NCC as super disintegrating agent and as solubility enhancer

3 EXPERIMANTAL WORK

3.1 PREPARATION, MODIFICATION AND CHARACTERIZATION OF SCBNCC, ITS APPLICATION AS A SOLUBILITY ENHANCER AND SUPER DISINTEGRATING AGENT

3.1.1 PREPARATION OF SCBNCC

SCBMCC was used as a starting material for the preparation of SCBNCC. Acid hydrolysis technique was used for the preparation of SCBNCC. 100 ml of (55 wt %) sulphuric acid solution at 55°C temperature with different reaction times of 90 min, under magnetic stirring was the condition used for the acid hydrolysis. SCBNCC suspension was collected and subjected to spray drying.

3.1.2 CHARACTERIZATION OF SCBNCC

SCBMCC and SCBNCC were characterized using various techniques like % yield, ATR-FTIR spectroscopy, SEM, TEM, TGA, and XRD.

3.1.3 MODIFICATION OF SCBNCC

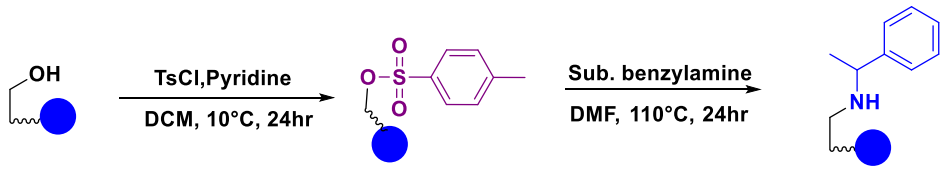

Figure 2 Reaction scheme for modification of SCBNCC

The modification reaction was completed in two steps. As shown in figure 2, Tosylation was done in the first step, which worked as a connecting chain for adding amines on the surface of SCBNCC. Briefly, 12.6 ml of dry pyridine and 10.5 ml of dry DCM were taken in two necked round bottom flask. p - toluene sulfonyl chloride was added drop wise in the RBF. 5 gm of SCBNCC was added, stirred for 10 min at RT, and the reaction was maintained below 10°C for 24 hrs. White solid precipitate was filtered and air dried, and ATR-FTIR was recorded for confirming the functional group change. The obtained intermediate was appropriately dried. An RBF with a condenser was charged with benzylamine 0.85 ml (0.015 mol), 2 g tosylate SCBNCC (0.007 mol), and 5 ml DMF. The reaction mixture was refluxed for 24 hr. at 110°C. The resulting mixture was filtered, dried under vacuum, and stored for further use.

3.1.4 CHARACTERIZATION OF MODIFIED SCBNCC

Modified SCBNCC was characterized using various techniques like ATR-FTIR spectroscopy, solid state NMR, TGA, and XRD.

3.1.5 OPTIMIZATION OF SCBNCC CONCENTRATION AND COMPRESSION FORCE BY USING DESIGN OF EXPERIMENTS

SCBNCC and modified SCBNCC were used as disintegrants. A full factorial design with two factors at 3-levels was used to optimize IR tablets (prepared using SCBNCC and modified SCBNCC individually). The matrix of experimental design comprises 9 trials and 3 center points. All the experimental batches were performed in triplicate, and the center points were repeated five times to decrease the possibility of errors. Analysis of variance (ANOVA) was used for statistical analysis using the design of the experiments. Polynomial equations were derived using DoE software, as shown in equations 2 –

$$Y = b_0 + b_1A_1 + b_2B_1 + b_{12}A_1B_2 + b_{11}A_{12} + b_{22}B_{22} \quad 1$$

Y represented the dependent variable, and b_0 was the arithmetic mean of 9 trials conducted as per DoE. A_1 and B_2 represent the primary two responses. A_{12} and B_{22} are polynomial terms. The significance of the model ($P<0.05$) and individual response parameters were estimated by one-way ANOVA.

Table 1 Design of experiments inputs

Factors	Levels			Dependent variables
	-1	0	+1	
SCBNCC and Modified SCBNCC (%) (used individually for optimization)	2.5	5	7.5	% Cumulative release Disintegration time
Compression force (tons)	2	4	6	

3.1.5.1 Determination of Disintegration time

The disintegration test apparatus was used to determine the disintegration time using purified water as the media. The media temperature was equilibrated at 37±2˚C, and one tablet was taken into each basket and rack assembly. The disk was used during the determination of the disintegration time of tablets. The time taken for tablet disintegration was noted, and the average and standard deviation were calculated (n = 6).

3.1.5.2 Determination of *In – vitro* dissolution performance

USP paddle type II apparatus was used for the dissolution study. A total number of 8 tablets were taken randomly from each batch. The dissolution test was done in 900 ml simulated intestinal fluid at 37±0.5˚C, and the paddle was operated at 50 rpm. Samples were withdrawn at 0, 5, 10, 15, 20, 30, 45, and 60 minutes and analyzed using UV spectrophotometry. The absorbance was taken at λ_{max} of 276 nm, and the concentration of the Diclofenac potassium was calculated.

3.1.6 PREPARATION OF DICLOFENAC POTASSIUM IR TABLETS PREPARED USING SCBNCC, MODIFIED SCBPNCC, MARKETED MCC, GODAVARI MCC, AND MARKETED NCC

Direct compression method was used to prepare immediate-release tablets. As mentioned in table 2, lactose, talc, and magnesium stearate were used as diluent, glidant, and anti–adherent, respectively. Active ingredients and other excipients were accurately weighed and mixed. The prepared mixtures were passed through 40 # sieve and then blended for 5 min. 100 mg tablets with a fixed weight, were directly compressed with pre-determined pressure ranging from 2-6 N. Direct compression is the tableting process of the blend, which excludes agglomeration or preliminary granulation process.

Table 2 Composition of Diclofenac potassium IR tablets

Ingredients (mg)	SCBNCC Batch	SCBNCC Batch	SCBNCC Batch	Modified SCBNCC Batch	Modified SCBNCC Batch	Modified SCBNCC Batch
Diclofenac potassium	50	50	50	50	50	50
Lactose	45	45	45	44	44	44
SCBNCC	3.5	3.5	3.5	-	-	-
Modified SCBNCC	-	-	-	4	4	4
Talc	1	1	1	1	1	1
Magnesium stearate	1	1	1	1	1	1
Total weight	100	100	100	100	100	100

3.1.6.1 COMPARISON OF DICLOFENAC POTASSIUM IR TABLETS PREPARED USING SCBNCC, MODIFIED SCBNCC, MARKETED MCC, GODAVARI MCC, MARKETED NCC AND COMMERCIAL PRODUCT

The optimized parameters were used for the compression of tablets using SCBNCC, modified SCBNCC, godavari MCC, marketed MCC, and marketed NCC as disintegrants. The tablets were evaluated and compared with marketed formulations (Cataflam) for disintegration time and dissolution studies.

Table 3 Composition of tablets prepared using SCBNCC

Ingredients (mg)	Batch 1	Batch 2	Batch 3	Batch 4
Diclofenac potassium	50	50	50	50
Lactose	44.5	44.5	44.5	44.5
SCBNCC	3.5	-	-	-
Godavari MCC	-	3.5	-	-
Marketed MCC	-	-	3.5	-
Marketed NCC	-	-	-	3.5
Talc	1	1	1	1
Magnesium stearate	1	1	1	1
Total weight	100	100	100	100

Table 4 Composition of tablets prepared using modified SCBNCC

Ingredients (mg)	Batch 1	Batch 2	Batch 3	Batch 4
Diclofenac potassium	50	50	50	50
Lactose	45	45	45	45
Modified SCBNCC	4	-	-	-
Godavari MCC	-	4	-	-
Marketed MCC	-	-	4	-
Marketed NCC	-	-	-	4
Talc	1	1	1	1
Magnesium stearate	1	1	1	1
Total weight	100	100	100	100

3.1.7 COMPARISON OF IVERMECTIN IR TABLETS PREPARED USING SCBNCC, MODIFIED SCBNCC, MARKETED MCC, GODAVARI MCC, AND MARKETED NCC

Tablets were prepared using SCBNCC, modified SCBNCC, marketed MCC, and marketed NCC and compared with a commercial product (Jetta 12).

Table 5 Composition of tablets prepared using SCBNCC

Ingredients (mg)	Batch 1	Batch 2	Batch 3	Batch 4
Ivermectin	12	12	12	12
Lactose	82.5	82.5	82.5	82.5
SCBNCC	3.5	-	-	-
Godavari MCC	-	3.5	-	-
Marketed MCC	-	-	3.5	-
Marketed NCC	-	-	-	3.5
Talc	1	1	1	1
Magnesium stearate	1	1	1	1
Total weight	100	100	100	100

Table 6 Composition of tablets prepared using modified SCBNCC

Ingredients (mg)	Batch 1	Batch 2	Batch 3	Batch 4
Ivermectin	12	12	12	12
Lactose	82	82	82	82
Modified SCBNCC	4	-	-	-
Godavari MCC	-	4	-	-
Marketed MCC	-	-	4	-
Marketed NCC	-	-	-	4
Talc	1	1	1	1
Magnesium stearate	1	1	1	1
Total weight	100	100	100	100

3.1.8 COMPARISON OF TICAGRELOR IR TABLETS PREPARED USING SCBNCC, MODIFIED BPNCC, MARKETED MCC, GODAVARI MCC, AND MARKETED NCC

Tablets were prepared using SCBNCC, modified SCBNCC, marketed MCC, marketed NCC and compared with a commercial product (Brilinta)

Table 7 Composition of tablets prepared using SCBNCC

Ingredients (mg)	Batch 1	Batch 2	Batch 3	Batch 4
Ticagrelor	90	90	90	90
Lactose	99	99	99	99
SCBNCC	7	-	-	-
Godavari MCC	-	7	-	-
Marketed MCC	-	-	7	-
Marketed NCC	-	-	-	7
Talc	2	2	2	2
Magnesium stearate	2	2	2	2
Total weight	200	200	200	200

Table 8 Composition of tablets prepared using modified SCBNCC

Ingredients (mg)	Batch 1	Batch 2	Batch 3	Batch 4
Ticagrelor	90	90	90	90
Lactose	98	98	98	98
Modified SCBNCC	8	-	-	-
Godavari MCC	-	8	-	-
Marketed MCC	-	-	8	-
Marketed NCC	-	-	-	8
Talc	2	2	2	2
Magnesium stearate	2	2	2	2
Total weight	200	200	200	200

3.1.9 COMPARISON OF RITONAVIR IR TABLETS PREPARED USING SBNCC, MODIFIED SCBNCC, MARKETED MCC, GODAVARI MCC, AND MARKETED NCC

Optimized SCBNCC, modified SCBNCC concentration, and process parameters were used to prepare Ritonavir IR tablets by direct compression methods. Tablets were prepared using SCBNCC, modified SCBNCC, marketed MCC, and marketed NCC compared with a commercial product (Norvir).

Table 9 Composition of tablets prepared using SCBNCC

Ingredients (mg)	Batch 1	Batch 2	Batch 3	Batch 4
Ritonavir	100	100	100	100
Lactose	89	89	89	89
SCBNCC	7	-	-	-
Godavari MCC	-	7	-	-
Marketed MCC	-	-	7	-
Marketed NCC	-	-	-	7
Talc	2	2	2	2
Magnesium stearate	2	2	2	2
Total weight	200	200	200	200

Table 10 Composition of tablets prepared using modified SCBNCC

Ingredients (mg)	Batch 1	Batch 2	Batch 3	Batch 4
Ritonavir	100	100	100	100
Lactose	88	88	88	88
Modified SCBNCC	8	-	-	-
Godavari MCC	-	8	-	-
Marketed MCC	-	-	8	-
Marketed NCC	-	-	-	8
Talc	2	2	2	2
Magnesium stearate	2	2	2	2
Total weight	200	200	200	200

3.2 PREPARATION, MODIFICATION AND CHARACTERIZATION OF BPNCC AND ITS APPLICATION AS SOLUBILITY ENHANCER AND SUPER DISINTEGRATING AGENT

3.2.1 PREPARATION OF BPNCC

Alkali treatment

The BPP was treated with 5% w/v NaOH at 1:50 solid-to-liquid ratio for removing lignin and hemicellulose. NaOH solution was taken in a beaker, and then BPP was added. The solution was stirred at 40°C for four h at 500 rpm. The solution was filtered, and the filter cake (remaining solid) was washed several times with Deionised (DI) water.

Bleaching treatment

After alkali treatment, the bleaching process was performed using 2% (w/v) sodium hypochlorite solution for two h at 40°C. The solid-to-liquid ratio was 1:10. The solution was filtered, and the solid obtained was washed several times with DI water till neutral pH was reached.

Acid hydrolysis

The dried bleached BPP obtained from the above process was subjected to acid hydrolysis with 200 mL of sulfuric acid (55% v/v) at 50°C for 60 min. After 60 min, a 10-time the volume of chilled DI water was added to the suspension to quench the hydrolysis reaction. The suspension was kept overnight in the refrigerator. The supernatant was decanted, and the pH of the solution was adjusted to 3 by repeated water washing followed by centrifugation at 6000X*g*. In the next step, the suspension was kept for dialysis for 5-6 days in distilled water to achieve a pH of 5. Finally, the suspension obtained was spray-dried, and the powder was stored in the refrigerator for further use.

3.2.2 CHARACTERIZATION OF BPNCC

BPP and spray-dried BPNCC were characterized using techniques such as TGA, ATR-FTIR, and XRD, FESEM and TEM as mention in section 3.1.2.

3.2.3 MODIFICATION OF BPNCC

As mentioned in section 3.1.3, the modification of BPNCC was performed.

3.2.4 CHARACTERIZATION OF MODIFIED BPNCC

As mentioned in section 3.1.4, modified BPNCC were characterized.

3.2.5 OPTIMIZATION OF BPNCC CONCENTRATION AND COMPRESSION FORCE BY USING DESIGN OF EXPERIMENT

As mentioned in section 3.1.5, the disintegrant (BPNCC and modified BPNCC) concentrations were optimized using the design of the experiments. Disintegrant concentration and compression force were taken as the factors, as shown in table 11.

Table 11 Inputs for design of experiments

Factors	Levels			Dependent variables
	-1	0	+1	
BPNCC and modified BPNCC (%) (used individually for optimization)	2.5	5	7.5	% Cumulative release Disintegration time
Compression force (ton)	2	4	6	

3.2.6 PREPARATION AND COMPARISON OF DICLOFENAC POTASSIUM IR TABLETS PREPARED USING BPNCC, MODIFIED BPNCC, MARKETED MCC, GODAVARI MCC, AND MARKETED NCC

IR tablets were prepared by direct compression methods, as mentioned in section 3.1.6. lactose, talc, and magnesium stearate were used as a diluent, glidants, and anti–adherent, respectively, as shown in table 12.

Table 12 Composition of Diclofenac potassium IR tablets

Ingredients (mg)	**BPNCC batch**	**BPNCC batch**	**BPNCC batch**	**Modified BPNCC batch**	**Modified BPNCC batch**	**Modified BPNCC batch**
Diclofenac potassium	50	50	50	50	50	50
Lactose	44.7	44.7	44.7	45.5	45.5	45.5
BPNCC	3.3	3.3	3.3	-	-	-
Modified BPNCC	-	-	-	2.5	2.5	2.5
Talc	1	1	1	1	1	1
Magnesium stearate	1	1	1	1	1	1
Total weight	100	100	100	100	100	100

3.2.7 COMPARISON OF DICLOFENAC POTASSIUM IR TABLETS PREPARED USING BPNCC, MODIFIED BPNCC, MARKETED MCC, GODAVARI MCC, AND MARKETED NCC

The optimized parameters were used for the compression of tablets using BPNCC, Modified BPNCC, godavari MCC, marketed MCC, and marketed NCC as disintegrants, as mentioned in tables 13 and 14. The tablets were evaluated and compared with marketed formulations for disintegration time and dissolution.

Table 13 Composition of tablets prepared using BPNCC

Ingredients (mg)	Batch 1	Batch 2	Batch 3	Batch 4
Diclofenac potassium	50	50	50	50
Lactose	44.7	44.7	44.7	44.7
BPNCC	3.3	-	-	-
Godavari MCC	-	3.3	-	-
Marketed MCC	-	-	3.3	-
Marketed NCC	-	-	-	3.3
Talc	1	1	1	1
Magnesium stearate	1	1	1	1
Total weight	100	100	100	100

Table 14 Composition of tablets prepared using modified BPNCC

Ingredients (mg)	Batch 1	Batch 2	Batch 3	Batch 4
Diclofenac potassium	50	50	50	50
Lactose	45.5	45.5	45.5	45.5
Modified BPNCC	2.5	-	-	-
Godavari MCC	-	2.5	-	-
Marketed MCC	-	-	2.5	-
Marketed NCC	-	-	-	2.5
Talc	1	1	1	1
Magnesium stearate	1	1	1	1
Total weight	100	100	100	100

3.2.8 COMPARISON OF IVERMECTI IR TABLETS PREPARED USING BPNCC, MODIFIED BPNCC, MARKETED MCC, GODAVARI MCC, AND MARKETED NCC

As mentioned in section 3.1.7, Ivermectin IR tablets were prepared by direct compression method. BPNCC, Modified BPNCC, Marketed MCC, Godavari MCC, and Marketed NCC were used as disintegrants to prepare each batch as mentioned in tables 15 and 16.

Table 15 Composition of tablets prepared using BPNCC

Ingredients (mg)	Batch 1	Batch 2	Batch 3	Batch 4
Ivermectin	12	12	12	12
Lactose	82.7	82.7	82.7	82.7
BPNCC	3.3	-	-	-
Godavari MCC	-	3.3	-	-
Marketed MCC	-	-	3.3	-
Marketed NCC	-	-	-	3.3
Talc	1	1	1	1
Magnesium stearate	1	1	1	1
Total weight	100	100	100	100

Table 16 Composition of tablets prepared using modified BPNCC

Ingredients (mg)	Batch 1	Batch 2	Batch 3	Batch 4
Ivermectin	12	12	12	12
Lactose	83.8	83.8	83.8	83.8
Modified BPNCC	2.5	-	-	-
Godavari MCC	-	2.5	-	-
Marketed MCC	-	-	2.5	-
Marketed NCC	-	-	-	2.5
Talc	1	1	1	1
Magnesium stearate	1	1	1	1
Total weight	100	100	100	100

3.2.9 COMPARISON OF TICAGRELOR IR TABLETS PREPARED USING BPNCC, MODIFIED BPNCC, MARKETED MCC, GODAVARI MCC, AND MARKETED NCC

As mentioned in section 3.1.8, Ticagrelor IR tablets were prepared by direct compression method. BPNCC, Modified BPNCC, Marketed MCC, Godavari MCC, and Marketed NCC were used as disintegrants to prepare each batch as mentioned in tables 17 and 18.

Table 17 Composition of tablets prepared using BPNCC

Ingredients (mg)	Batch 1	Batch 2	Batch 3	Batch 4
Ticagrelor	90	90	90	90
Lactose	99.4	99.4	99.4	99.4
BPNCC	6.6	-	-	-
Godavari MCC	-	6.6	-	-
Marketed MCC	-	-	6.6	-
Marketed NCC	-	-	-	6.6
Talc	2	2	2	2
Magnesium stearate	2	2	2	2
Total weight	200	200	200	200

Table 18 Composition of tablets prepared using modified BPNCC

Ingredients (mg)	Batch 1	Batch 2	Batch 3	Batch 4
Ticagrelor	90	90	90	90
Lactose	101	101	101	101
Modified BPNCC	5	-	-	-
Godavari MCC	-	5	-	-
Marketed MCC	-	-	5	-
Marketed NCC	-	-	-	5
Talc	2	2	2	2
Magnesium stearate	2	2	2	2
Total weight	200	200	200	200

3.2.10 COMPARISON OF RITONAVIR IR TABLETS PREPARED USING BPNCC, MODIFIED BPNCC, MARKETED MCC, GODAVARI MCC, AND MARKETED NCC

As mentioned in section 3.1.9, Ritonavir IR tablets were prepared by direct compression method. BPNCC, modified BPNCC, marketed MCC, godavari MCC, and marketed NCC were used as disintegrants to prepare each batch as mentioned in tables 19 and 20.

Table 19 Composition of tablets prepared using BPNCC

Ingredients (mg)	Batch 1	Batch 2	Batch 3	Batch 4
Ritonavir	100	100	100	100
Lactose	89.4	89.4	89.4	89.4
BPNCC	6.6	-	-	-
Godavari MCC	-	6.6	-	-
Marketed MCC	-	-	6.6	
Marketed NCC	-	-	-	6.6
Talc	2	2	2	2
Magnesium stearate	2	2	2	2
Total weight	200	200	200	200

Table 20 Composition of tablets prepared using modified BPNCC

Ingredients (mg)	Batch 1	Batch 2	Batch 3	Batch 4
Ritonavir	100	100	100	100
Lactose	91	91	91	91
Modified BPNCC	5	-	-	-
Godavari MCC	-	5	-	-
Marketed MCC	-	-	5	
Marketed NCC	-	-	-	5
Talc	2	2	2	2
Magnesium stearate	2	2	2	2
Total weight	200	200	200	200

4 RESULTS AND DISCUSSION

4.1 PREPARATION, MODIFICATION AND CHARACTERIZATION OF SCBNCC, ITS APPLICATION AS SOLUBILITY ENHANCER AND SUPER DISINTEGRATING AGENT

4.1.1 PREPARATION OF SCBNCC FROM SCBMCC

SCBNCC was successfully prepared from SCBMCC using acid hydrolysis technique. The minimum size of SCBNCC was obtained with the conditions 55 %v/v of acid concentration, 1000 rpm at 55°C temperature.

4.1.2 CHARACTERIZATION OF SCBNCC

SCBMCC and SCBNCC were characterized using various techniques like % yield, ATR-FTIR spectroscopy, SEM, TEM, TGA, and XRD.

4.1.2.1 SCBNCC % Yield

The isolated SCBNCC yield is 35.5%. The experimental trials showed the highest yield when the reaction time was 90 min at 55% sulfuric acid concentration with a stirring speed of 1000 rpm.

4.1.2.2 Morphology and Particle size analysis

Scanning Electron Microscopy

SEM images of SCBNCC prepared from SCBMCC are shown in figure 3. Results clearly showed a smooth, long fibrous structure. Interestingly, SCBNCC displayed an irregular rod-like rather than a nano needle-like shape. It might be due to tiny nano fragments that agglomerate with elementary SCBNCC crystallites by interfacial hydrogen bond.

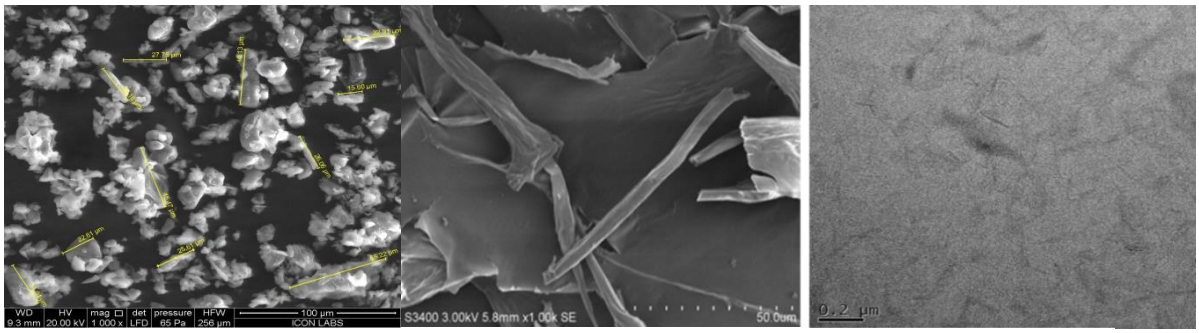

A B C

Figure 3 A- SEM images of SCBMCC, B- SEM image of SCBNCC, C- TEM image of SCBNCC

4.1.2.3 ATR-FTIR Analysis

Infrared spectra of SCBMCC and SCBNCC are given in figure 4. There is no significant difference in the spectra as SCBMCC was already processed MCC and was prepared after removing lignin and hemicellulose. An almost similar spectrum was observed in SCBMCC and SCBNCC, with reduced sharpness showing no change in the functional groups.

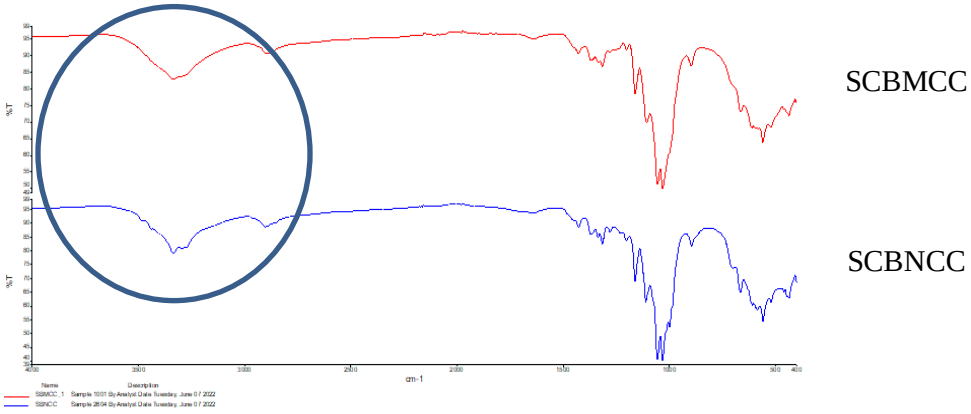

Figure 4 ATR-FTIR spectra of SCBNCC and SCBMCC

4.1.2.4 Thermal properties

Thermal degradation properties of prepared SCBNCC and SCBMCC were measured by thermo gravimetric analysis. As illustrated in figure 5, samples have mainly two-step weight change. The degradation stages of Sugarcane bagasse SCBMCC and SCBNCC start from 310.23°C - 344.46°C and 252.22°C - 283.53°C respectively. In both spectra, an initial weight loss below 100°C showed water evaporation contributed to the hydrophilic character of the lignocellulose fibers.

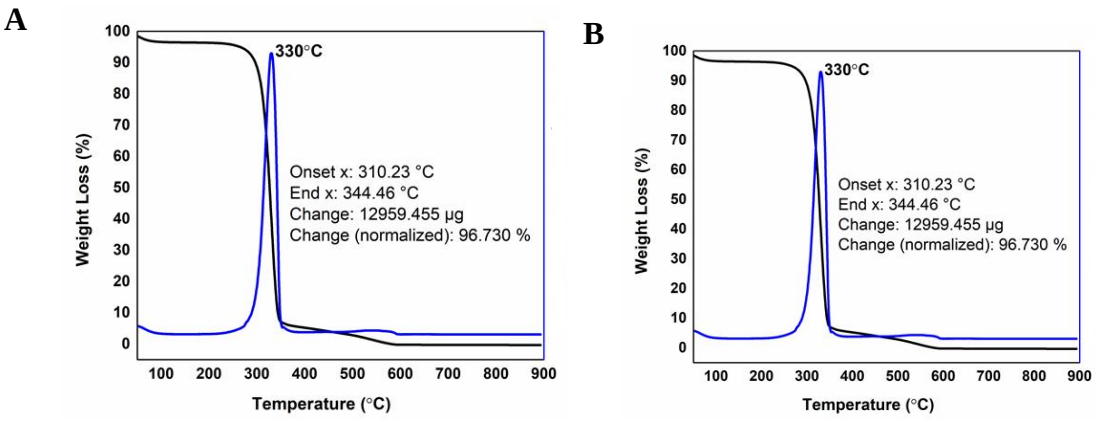

Figure 5 TGA curves of SCBMCC (A) and SCBNCC (B)

4.1.2.5 XRD of SCBNCC

The XRD patterns of SCBMCC and SCBNCC are shown in figure 6. The crystallinity index calculated by Segal method was found to be 64% with its highly intense peak at 22.8°, whereas MCC showed 52% crystallinity. This indicated that sugarcane bagasse-derived MCC was a reliable cellulose source for obtaining NCC with higher crystallinity.

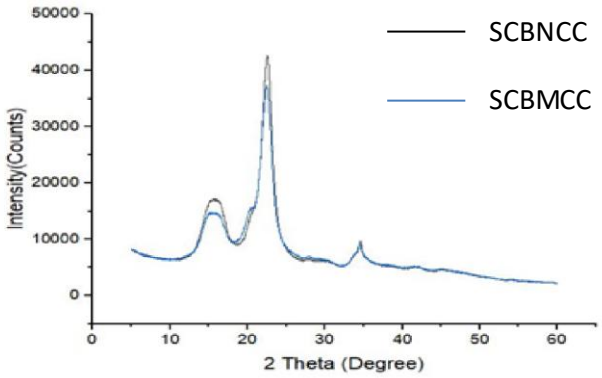

Figure 6 X-ray diffractogram of SCBMCC and SCBNCC

4.1.3 CHARACTERIZATION OF SURFACE MODIFIED-SCBNCC

4.1.3.1 ATR-FTIR spectroscopy

ATR-FTIR spectra of the SCBNCC and modified SCBNCC are shown in figure 7. ATR-FTIR spectra of the SCBNCC and modified SCBNCC showed peaks in two regions – 3385 cm-^{1} and at 3210 cm-^{1} which shows presence of amine in modified SCBNCC. The result proved that the modified SCBNCC amination was completed successfully.

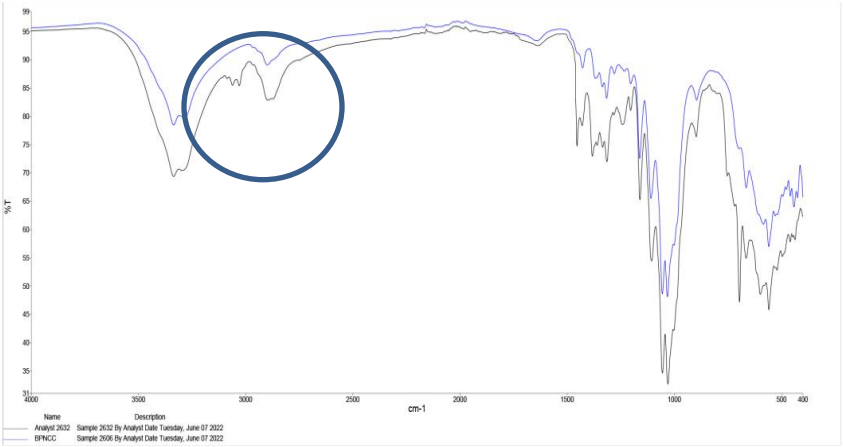

Figure 7 ATR-FTIR spectra of SCBNCC and modified SCBNCC

4.1.3.2 Solid state ^{13}C NMR spectroscopy

The peaks in solid state ^{13}C NMR spectra of SCBNCC were extended over a chemical shift

from 57 to 108 ppm and divided into four separate regions, resolved to a different extent, including less resolved regions C6 (58–69 ppm), C1 (102–108 ppm) and C2,3,5 in the cellulosic ring (70–80 ppm), and well resolved region C4 (80–92 ppm). Similar kind of spectrum was obtained in modified SCBNCC, which showed the intact SCBNCC structure. A region between 120-130 ppm showed presence of aromatic ring and chemical shift below 50 ppm showed presence of alkane.

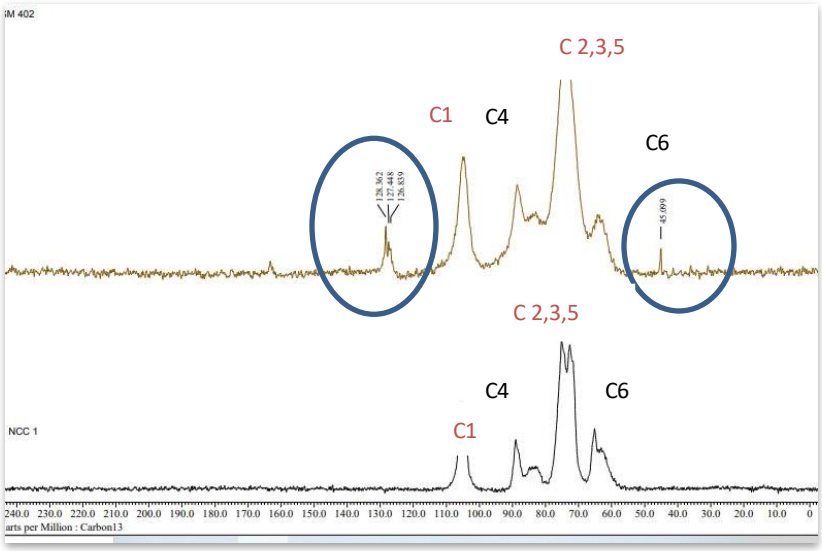

Figure 8 ^{13}C solid-state NMR spectra of modified SCBNCC and SCBNCC

4.1.3.3 Thermal properties

The thermal degradation property of modified SCBNCC was measured by thermo gravimetric analysis in a range of temperatures (0 to 900°C) under an inert atmosphere. In TGA, the first degradation peaks start at 150°C, which is due to the departure of water. -210°C, second degradation starts at 270-380°C with the peak at 369.4°C (total mass loss 97). The result indicated that the modified SCBNCC shows optimal thermal stability.

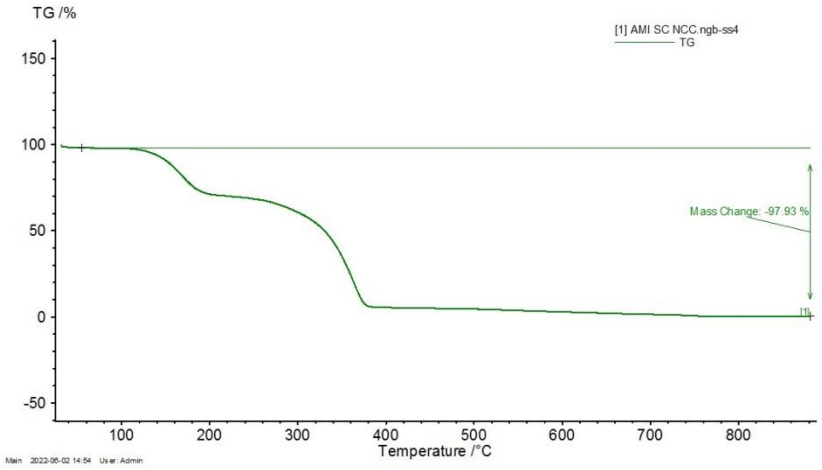

Figure 9 TGA curve of modified SCBNCC

4.1.3.4 XRD of modified SCBNCC

The XRD pattern of modified SCBNCC is shown in the figure 10. The result showed crystallinity of SCBNCC was maintained after the modification. No prominent diffraction peak confirmed no significant change in NCC nature.

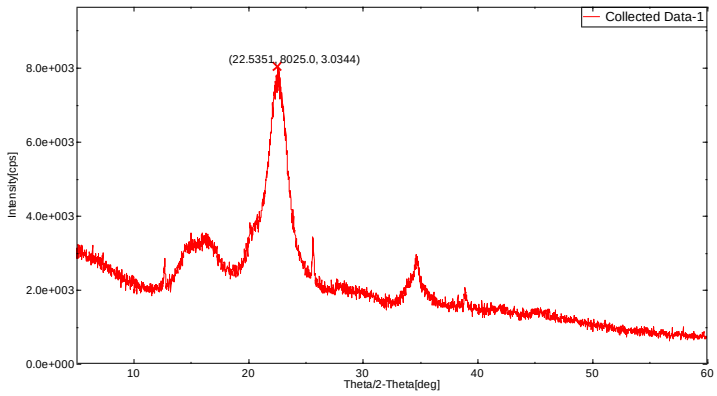

Figure 10 XRD diffractogram of modified SCBNCC

4.1.4 OPTIMIZATION OF SCBNCC CONCENTRATION

4.1.4.1 Optimization of SCBNCC concentration and compression force by using design of experiments

DOE studies were performed using full factorial 3^2 design of response surface methodology for optimizing the material and process parameters. A total number of 9 experimental runs and 3 central runs were designed considering two independent factors, namely, the concentration of disintegration (%) and compression force (N).

4.1.4.2 Determination of Disintegration time

As mentioned earlier under section 3.1.5.1, the disintegration time was found to be 318-445 seconds. The observations of disintegration time were recorded.

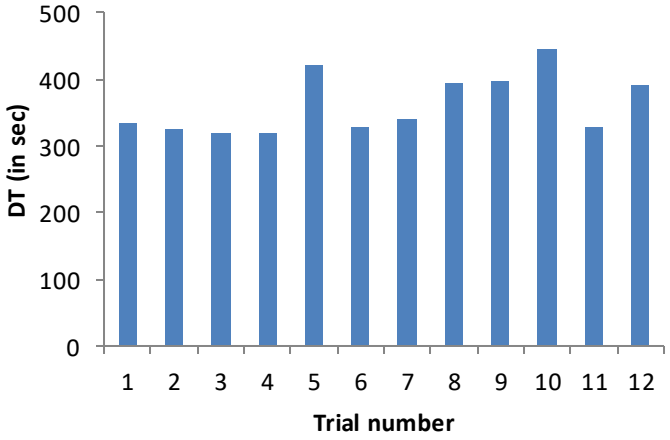

Figure 11 Disintegration time for all trial batches

Determination of % cumulative drug release

As mentioned earlier under section 3.1.5.2, the % cumulative release was found to be 78.3-89.9. Analysis of both the responses was performed using ANOVA without any power transformation. The results of the statistical analysis are summarized in table 21. All the two reduced models demonstrated p-values less than 0.05 and F-values higher than those of the respective full models and were significant. The lack of fit of F-values for the reduced model was insignificant, indicating that the models fit the data. The R^2 value calculated for disintegration time and % cumulative release was more than 0.7, which suggested a robust model fit for both responses. Moreover, the adequate precision values were more significant than 4 for all the two reduced models, indicating a sufficient signal-to-noise ratio. Both the polynomial equations are given in table 21. Software-generated contour plots and 3D surface plots are shown in figure 12. The correlation of the concentration of SCBNCC and compression force to DT and % cumulative release was nonlinear.

Table 21 Summary of statistical analysis of responses using ANOVA

A. Calculated Statistical values:							
Sr. No.	Response	Reduced model	P-value	F-value	Lack of fit F-value	Correlation coefficient (R^2)	Adequate precision
1	Disintegration time	Quadratic	<0.0001	40.77	2.99	0.9588	18.6078
2	% cumulative release	Quadratic	<0.0001	208.62	0.0429	0.9917	42.4234
B. Polynomial equations:							
1	Disintegration time = +483.67 +246 A + 34B + 92 A^2 + 41B^2						
2	% cumulative release = +78.57 - 15.37A – 2.45B – 5.25A^2 -4.26B^2						

Optimized formulation, goals for responses were set as minimum disintegration time and maximum drug release. A numerical solution with the highest desirability, i.e., 1, was considered. A design space was defined from the overlay of contour plots of both the two responses for factor A and factor B. The optimized formulation was suggested to contain 3.5% SCBNCC concentration at the compression force of 3 N. The corresponding results were compared with the goals for responses. The characteristics of optimized formulation showed 313-second disintegration and 90.2 % cumulative release.

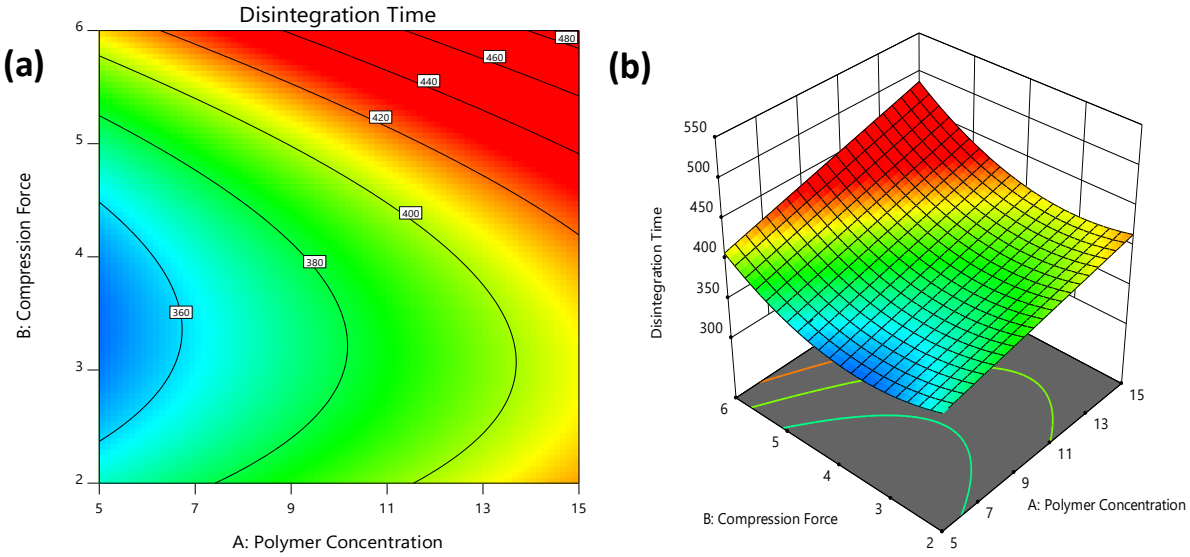

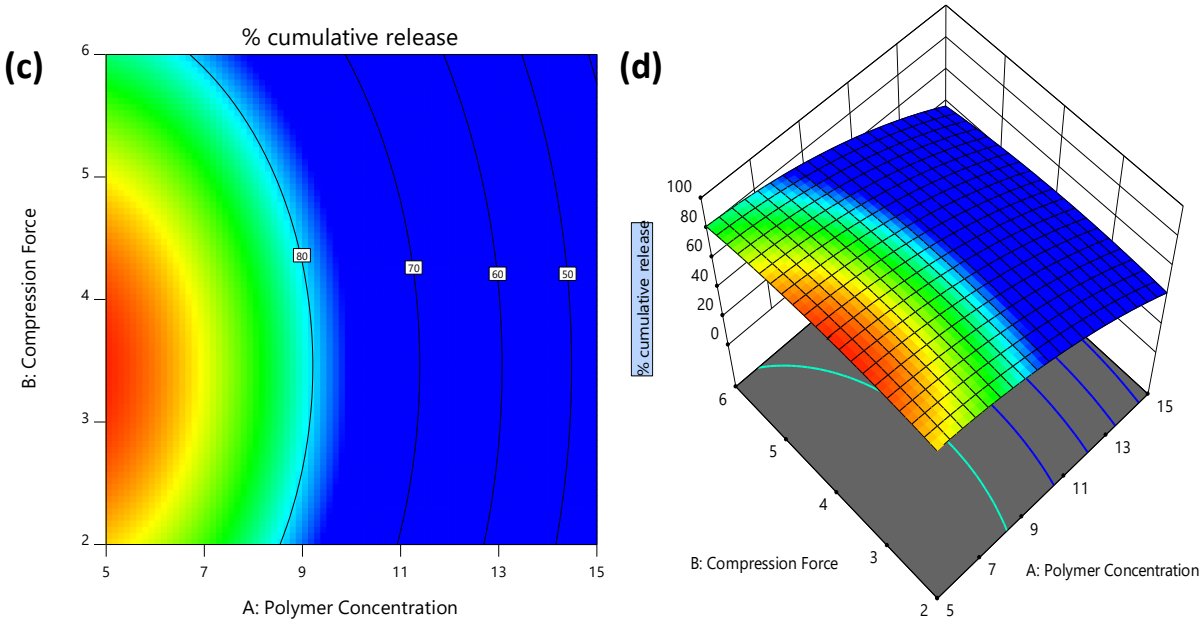

Figure 12 Contour (a,c) and 3D surface (b, d) plots demonstrating nonlinear correlation of factor A and B with both responses: (a-c) % cumulative release, (c-d) DT

4.1.5 OPTIMIZATION OF MODIFIED SCBNCC CONCENTRATION

4.1.5.1 Optimization of Modified SCBNCC concentration and compression force by using design of experiments

A total number of 9 experimental runs and 3 central runs were designed considering two independent factors, namely, the concentration of modified SCBNCC (%) and compression force (N). Every factor was considered at three levels, the actual values given in table 10. Disintegration time and % cumulative release were selected as responses, i.e., measurable dependent variables. Tablets compressed with modified SCBNCC were characterized as per DOE protocol.

4.1.5.2 Determination of Disintegration time

The disintegration time was found to be 180-265 seconds. The observations of disintegration time recorded for designed 12 experimental runs are compiled in figure 13.

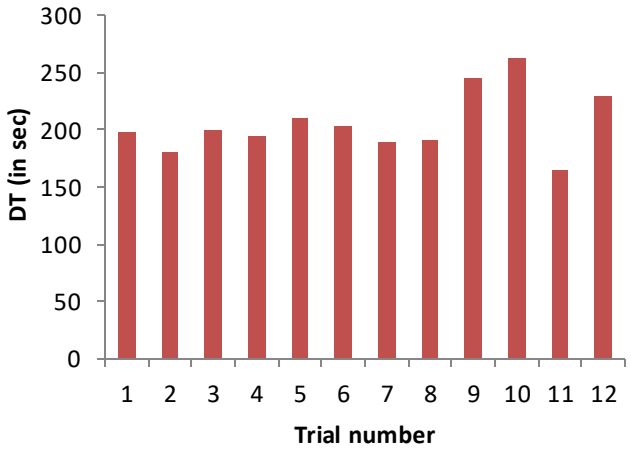

Figure 13 Disintegration time of trial batch

4.1.5.3 Determination of % cumulative drug release

As mentioned earlier under section 3.1.5.2, % cumulative release was found to be 85-99.5. Analysis of both the responses was performed using ANOVA without any power transformation. The results of the statistical analysis are summarized in table 22. Both the polynomial equations are given in table 22. Software-generated contour plots and 3D surface plots are shown in figure 14. The correlation of the concentration of modified SCBNCC and compression force to DT and % cumulative release was nonlinear.

Table 22 Summary of statistical analysis of responses using ANOVA

A. Calculated Statistical values:							
Sr. No.	Response	Reduced model	P-value	F-value	Lack of fit F-value	Correlation coefficient (R^2)	Adequate precision
1	Disintegration time	Quadratic	< 0.0001	244.10	0.4538	0.9892	48.18
2	% cumulative release	Quadratic	0.0001	29	0.5222	0.9158	17.30
B. Polynomial equations:							
1	Disintegration time = +319.50 +173.67 A + 13.50 B + 53.33 A^2						
2	% cumulative release = +85.63 – 25.17 A – 3.75 B – 13.80 A^2						

To finalize the optimized formulation, goals for responses were set as minimum disintegration time and maximum drug release. A numerical solution with the highest desirability, i.e., 1 was considered. A design space was defined from the overlay of contour plots of the two responses for factor A and factor B. The optimized formulation was suggested to contain 4.1% modified SCBNCC concentration at the compression force 2 N.

The corresponding results were compared with the goals for responses. The characteristics of optimized formulation showed 175.5 seconds DT and 99.9 % cumulative release.

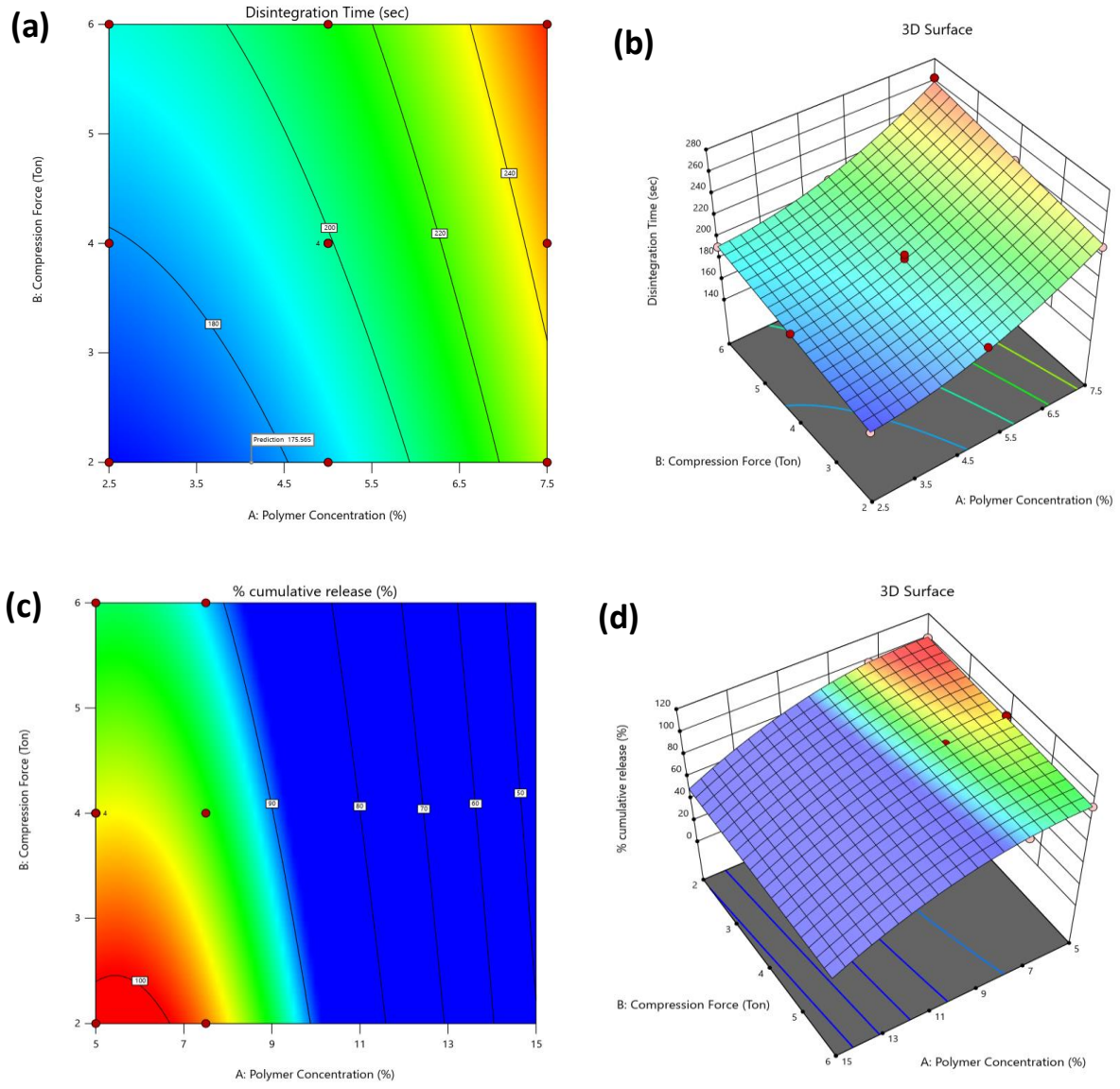

Figure 14 Contour (a, c) and 3D surface (b, d) plots demonstrating the non-linear correlation of factor A and B with two responses: (a-c) % cumulative release, (b-d) DT

4.1.6 COMPARISON OF DICLOFENAC POTASSIUM IR TABLETS PREPARED USING SCBNCC, MODIFIED SCBNCC, MARKETED MCC, GODAVARI MCC, AND MARKETED NCC

The tablets were compressed at 3.5 N using 3.5% SCBNCC concentration. 4% modified SCBNCC was used and tablets were compressed at 2 N. All the tablets were evaluated for disintegration time and % cumulative release. SCBNCC and modified SCBNCC tablets were compared to other tablets. Results showed that modified cellulose tablets have lesser DT compared to others.

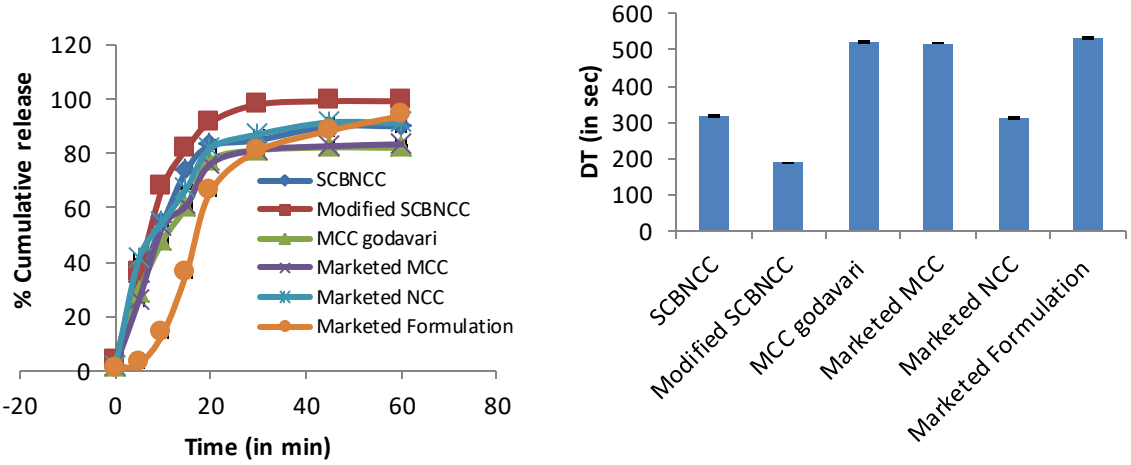

Figure 15 Comparison of in-vitro dissolution study and DT of Diclofenac potassium tablets prepared with different disintegrants

The dissolution profile of diclofenac potassium is shown in figure 15. Dissolution profile of the all tablets compared and found that modified SCBNCC tablets showed highest release among all tablets which is around 99%, SCBNCC showed 89.9 % of drug release. Modified SCBNCC tablets disintegrated within 190 seconds which was the fastest DT obtained when compared with other disintegrant tablets and marketed formulations. The increase in the dissolution of tablets was possibly a result of adding primary amino acid on the surface of nanocrystalline cellulose, thus improving the wettability and dissolution of tablets.

4.1.7 COMPARISON OF IVERMECTIN IR TABLETS PREPARED USING SCBNCC, MODIFIED SCBNCC, MARKETED MCC, GODAVARI MCC, AND MARKETED NCC

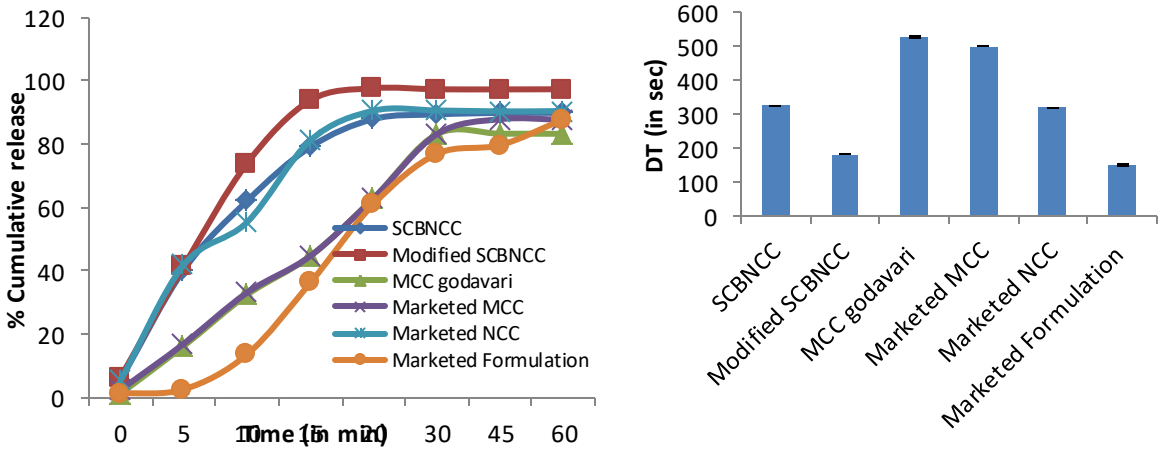

Figure 16 Comparison of in-vitro dissolution study and DT of Ivermectin tablets prepared with different disintegrants

Modified SCBNCC showed 97.3% drug release which is highest among all formulations and lowest release was found to be with MCC godavari as disintegrant, which is 83%. As shown in figure 16, modified SCBNCC showed the lowest DT among all the tablets which was around 180 seconds.

4.1.8 COMPARISON OF TICAGRELOR IR TABLETS PREPARED USING SCBNCC, MODIFIED SCBNCC, MARKETED MCC, GODAVARI MCC, AND MARKETED NCC

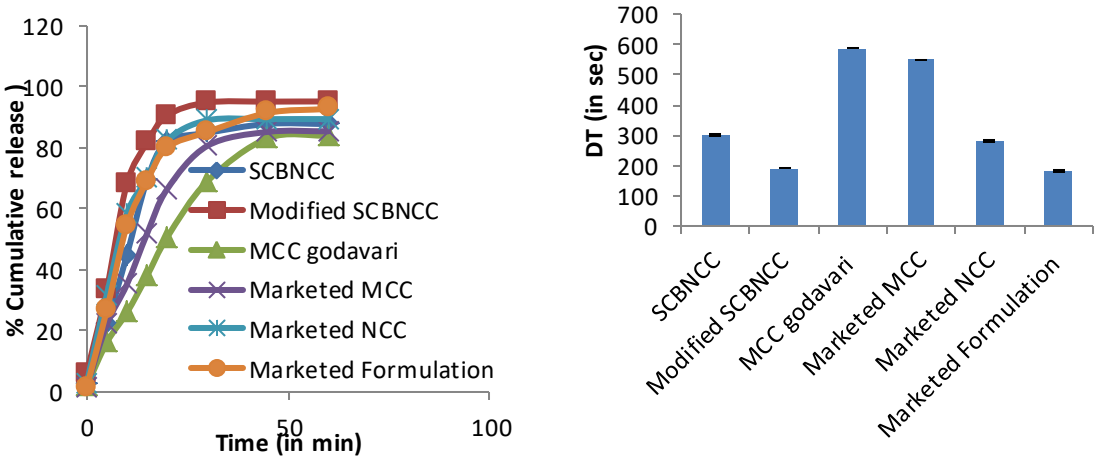

Figure 17 Comparison of in-vitro dissolution study and DT of Ticagrelor tablets prepared with different disintegrants

Modified SCBNCC showed 96% of drug release which is highest among all formulations and lowest release was found to be with MCC godavari as disintegrants 75%. The lowest DT was showed by modified SCBNCC around 191 seconds and the highest was obtained with SCBMCC which was 588 seconds.

4.1.9 COMPARISON OF RITONAVIR IR TABLETS PREPARED USING SCBNCC, MODIFIED SCBNCC, MARKETED MCC, GODAVARI MCC, AND MARKETED NCC

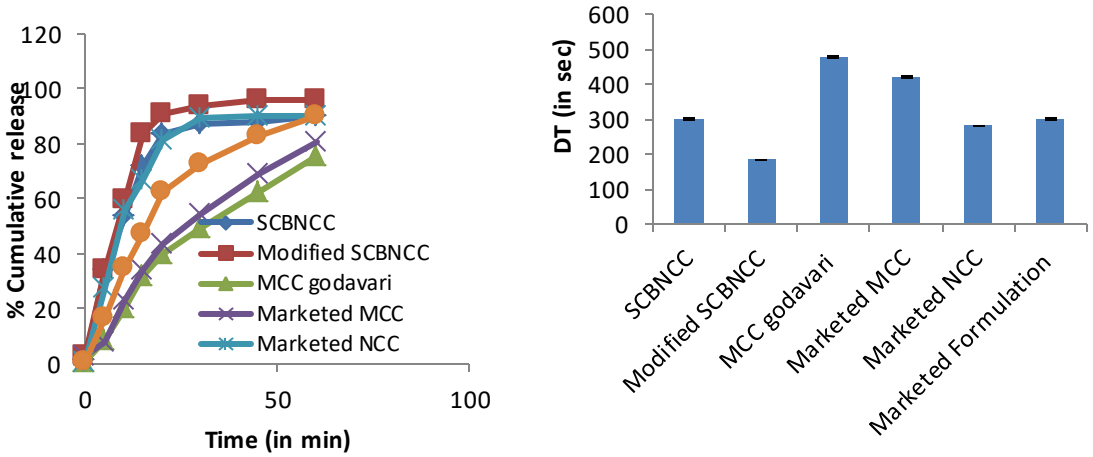

Figure 18 Comparison of in-vitro dissolution study and DT of Ritonavir tablets prepared with different disintegrants

Modified SCBNCC showed 95.9% drug release which is highest among all formulations and lowest release found to be 75.3% with MCC godavari as disintegrants. The lowest DT was showed by modified SCBNCC around 185 seconds and the highest was obtained with SCBMCC which was 478.5 seconds.

4.2 PREPARATION, MODIFICATION AND CHARACTERIZATION OF BPNCC AND ITS APPLICATION AS SOLUBILITY ENHANCER AND SUPER DISINTEGRATING AGENT

BPNCC was successfully prepared from BPP using aid hydrolysis and characterized further.

4.2.1 CHARACTERIZATION OF BPNCC

4.2.1.1 % Yield of BPNCC

The isolated BPNCC yield was found to be 29.9%.

4.2.1.2 Morphological investigation

Microscopic evaluation, FESEM, and TEM images (figure 19) of BPNCC showed needle-shaped crystals with a smooth surface compared to BPP images. It has a diameter of around 15-20 nm, and length is around 100-200 nm.

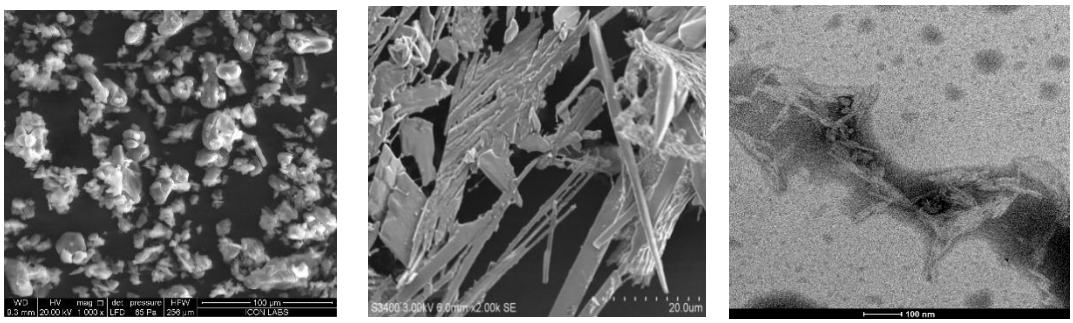

A B C

Figure 19 A - SEM Images of BPP, B- SEM image of BPNCC, and C- TEM images of BPNCC

4.2.1.3 ATR- FTIR spectroscopy

ATR FT-IR of BPP and BPNCC (figure 20) showed a broad peak located in the range of 3450–3300 cm^{-1}. This was observed in both the spectra which are representative of O-H bond stretching. Compared to BPP, at 3347 cm^{-1} intense peak was observed in NCC due to hydrolysis, which reflects hydrophilic properties. The peaks observed at 2919 and 2850 cm^{-1} in BPNCC were due to the stretching of H groups and aliphatic saturated C-H, respectively. In BPP, the peaks observed in the range of 1700–1450 cm^{-1} are assigned to the C=O stretching, C=C vibration of aromatic skeletal. This peak is absent in BPNCC due to the total removal of lignin and hemicellulose.

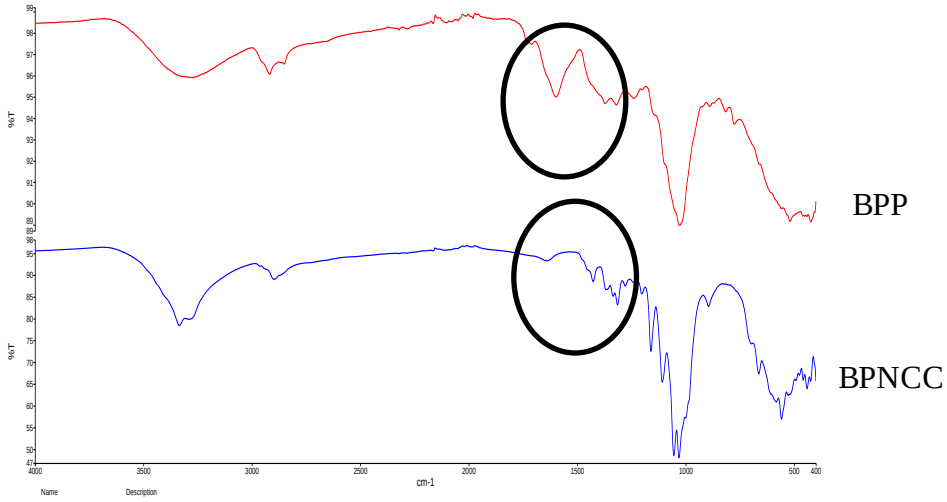

Figure 20 ATR-FTIR spectra of BPP and BPNCC

4.2.1.4 Thermal properties

Thermal analysis of BPP and BPNCC was performed to check the thermal stability of the compound. As shown in figure 21 three step degradations were found in both the thermograms. An initial weight loss below 100°C was observed in BPP and BPNCC which is water evaporation due to the hydrophilic character of lignocellulose fibers. In case of BPP, at higher temperatures, a sharp weight drop was observed due to the decomposition of the glycosyl unit present in cellulose fiber, which shows the presence of hemicellulose, lignin, and pectin. In BPP, there was a weight loss peak at 450°C, which showed the presence of lignin. This is not seen in the BPNCC thermogram, which indicates complete removal of lignin after hydrolysis.

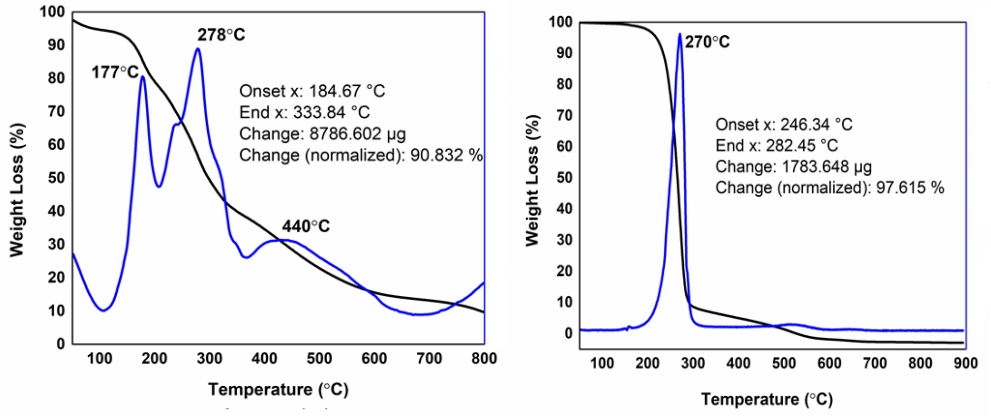

Figure 21 TGA curves of BPP and BPNCC

4.2.1.5 XRD of BPNCC

XRD analysis was performed to evaluate the crystallinity of BPP and BPNCC, as shown in figure 22. The crystallinity index obtained for NCC was 62.18%, displaying the strongest and highest peak at 2θ = 19° and 22.2°. The increased crystallinity is due to the removal of lignin and hemicellulose after hydrolysis, which caused the realignment of cellulose. During hydrolysis, hydronium ion penetrates and promotes hydrolytic cleavage of β-1, 4-glucopyranose bonds, making it more crystalline.

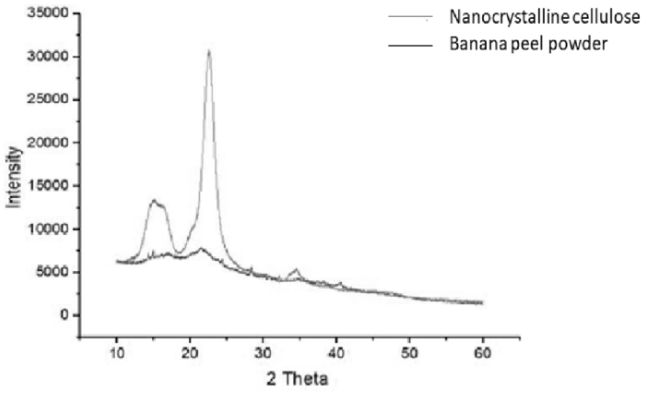

Figure 22 X-ray diffractogram of BPP and BPNCC

4.2.2 CHARACTERIZATION OF SURFACE MODIFIED-BPNCC

4.2.2.1 ATR-FTIR spectroscopy

ATR-FTIR spectra of the BPNCC and modified BPNCC showed peaks in two regions – 3361 cm^{-1} and at 3206 cm^{-1} which shows presence of amine in BPNCC. These results proved that BPNCC amination was obtained successfully in the selected reaction conditions.

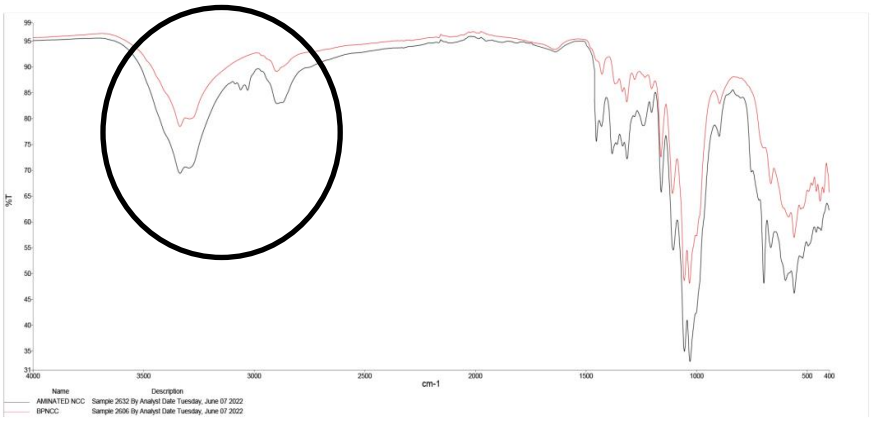

Figure 23 ATR-FTIR spectra of BPNCC and modified BPNCC

4.2.2.2 Solid state C^{13} NMR spectroscopy

The peaks in solid state ^{13}C NMR spectra of BPNCC were extended over a chemical shift from 57 to 108 ppm and divided into four separate regions, resolved to a different extent, including less resolved regions C6 (58–69 ppm), C1 (102–108 ppm) and C2,3,5 in the cellulosic ring (70–80 ppm), and well resolved region C4 (80–92 ppm). Ultra-structural information regarding crystallinity could be extracted from the C4 peak in the isolated cellulose spectrum, which is resolved into crystalline. One study showed, higher peak intensity of C1 and C4 is corresponding to crystallinity of NCC. Similar kind of spectra was obtained in modified BPNCC, which showed the intact BPNCC structure.

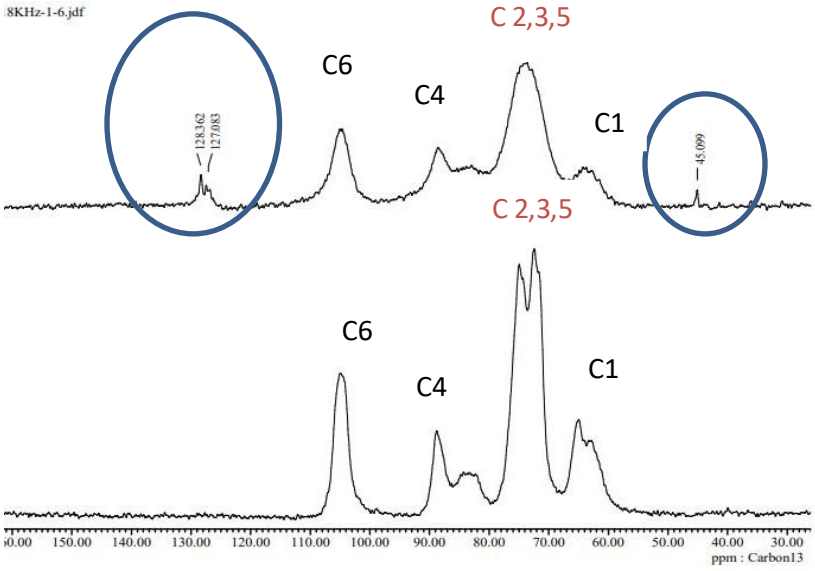

Figure 24 ^{13}C NMR of BPNCC and modified BPNCC

4.2.2.3 Thermal properties

The thermal degradation property of modified BPNCC was measured by thermo gravimetric analysis in the range of temperatures (0 to 900°C) under an inert atmosphere. In TGA, the first degradation starts at 270-410°C and peaks at 267.2°C (total mass loss 99%). The result showed that modified BPNCC has good thermal stability.

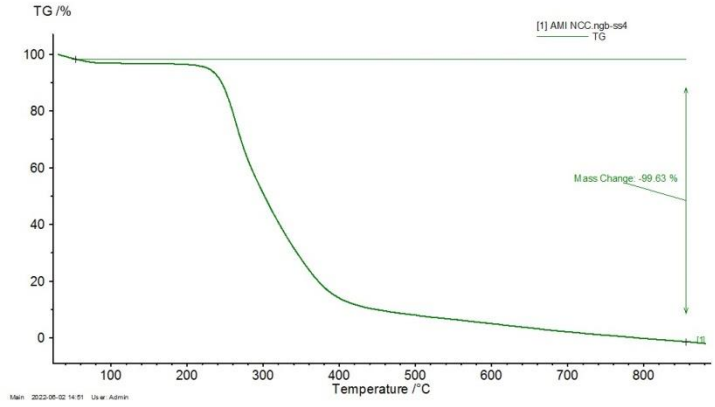

Figure 25 TGA curves of modified BPNCC

4.2.2.4 XRD of modified BPNCC

The XRD pattern of modified BPNCC is shown in the figure 26. The results showed that there was no prominent diffraction peak after modification confirming no significant change in BPNCC nature.

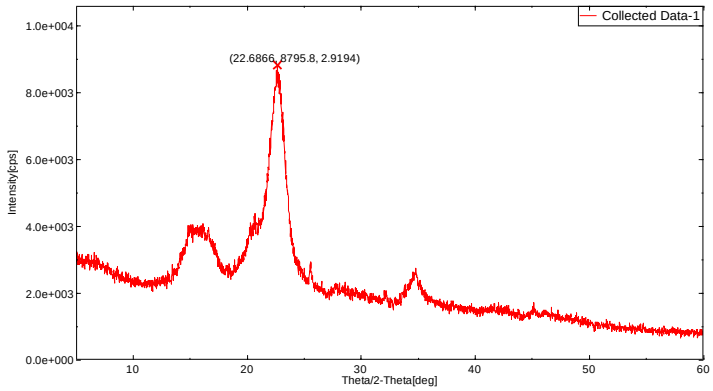

Figure 26 XRD diffractogram of modified BPNCC

4.2.3 OPTIMIZATION OF BPNCC CONCENTRATION

4.2.3.1 Optimization of BPNCC concentration and compression force by using design of experiments

A total number of 9 experimental runs and 3 central runs were designed considering two independent factors, namely, the concentration of disintegration (%) and compression force (N). Every factor was considered at three levels, as per the actual values mentioned in table 4.5. DT and % cumulative release were selected as responses, i.e., measurable dependent variables. Tablets compressed with BPNCC as disintegrant were used and characterized as per DOE protocol.

4.2.3.2 Determination of Disintegration time

As mentioned earlier under section 3.2.5.1, the disintegration time was found to be 318-345 seconds. The observations of disintegration time recorded for designed 12 experimental runs are compiled in figure 27.

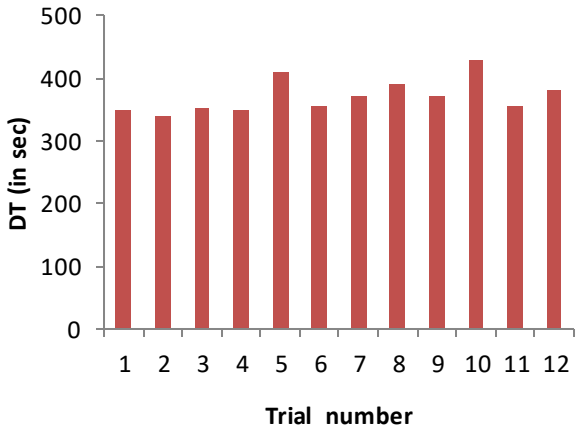

Figure 27 Disintegration time of DoE trial batches

4.2.3.3 Determination of % cumulative drug release

As mentioned earlier under section 3.2.5.2, % cumulative release was found to be in the range of 78-89.9. Analysis of both the responses was performed using ANOVA without any power transformation. The results of statistical analysis are summarized in table 23. Software-generated contour plots and 3D surface plots are shown in figure 28. The correlation of concentration of BPNCC and compression force to DT and % cumulative release was nonlinear.

Table 23 Summary of statistical analyses of responses using ANOVA

A. Calculated Statistical values:							
Sr. No.	Response	Reduced model	p-value	F-value	Lack of fit F-value	Correlation coefficient (R^2)	Adequate precision
1	Disintegration time	Quadratic	<0.0001	383.42	0.9104	0.9955	62.3158
2	% cumulative release	Quadratic	0.0002	29.43	3.92	0.9439	15.0572
B. Polynomial equations:							
1	Disintegration time = +384.50 +31.67 A + 28.33B + 7.50 AB + 36.33B^2						
2	% cumulative release = +76 - 21.87A – 2.47B – 8.90A^2 -4.52B^2						

To identify the optimized formulation, goals for responses were set as minimum disintegration time and maximum drug release. A numerical solution with the highest desirability, i.e., 1 was considered. A design space was defined from the overlay of contour plots of both the responses for factor A and factor B. The optimized formulation was suggested to contain 3.3% of BPNCC concentration at the compression force 3 N. The corresponding results were compared with the goals for responses. The characteristic of optimized formulation showed 313 second disintegration and 90.2 % cumulative release.

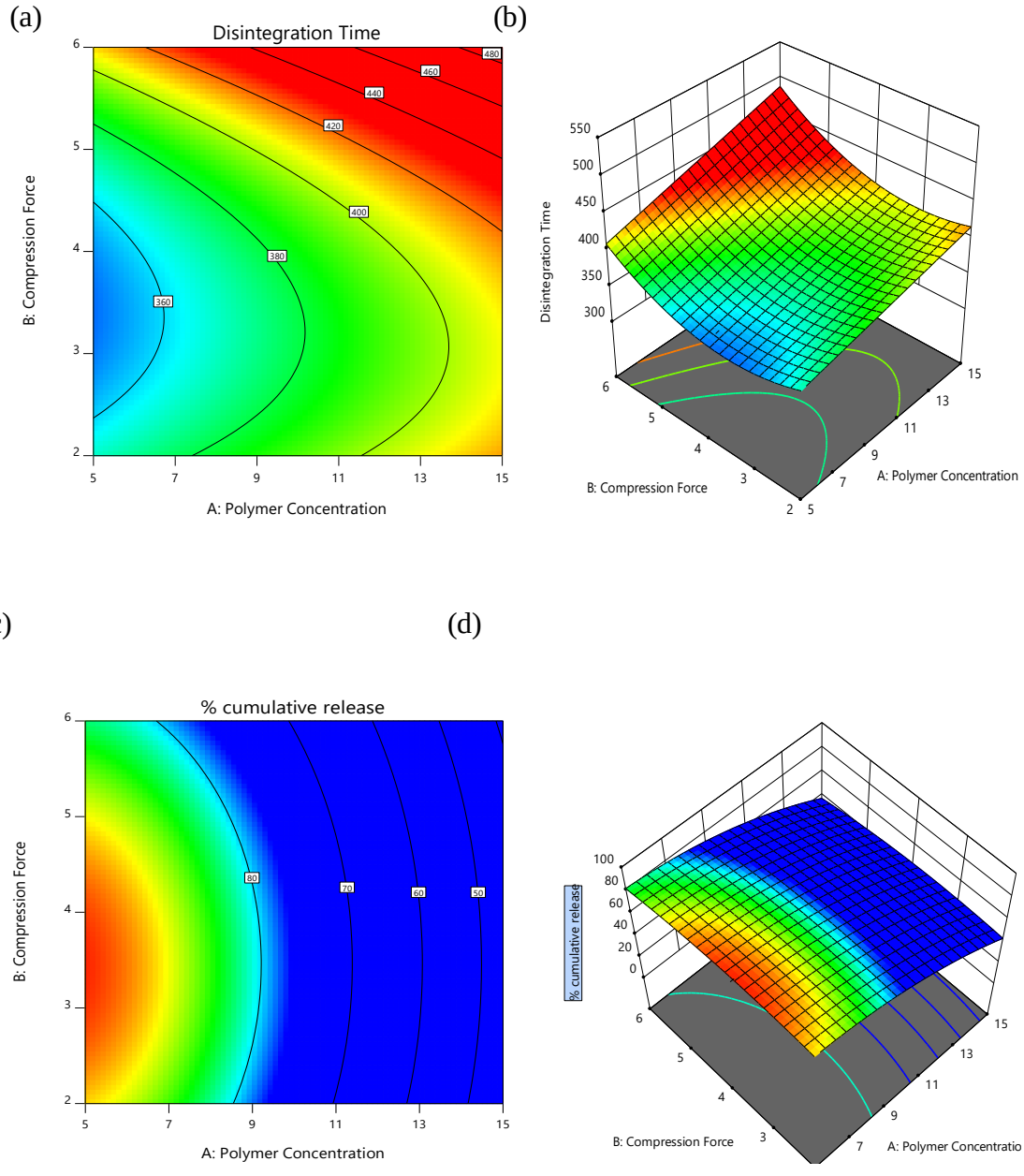

Figure 28: Contour (a,c) and 3D surface (b, d) plots to demonstrate the nonlinear correlation of factor A and factor B with all two responses: (a-b) DT, (c-d) % cumulative release

4.2.4 OPTIMIZATION OF CONCENTRATION OF MODIFIED BPNCC

4.2.4.1 Optimization of Modified BPNCC concentration and compression force using DoE

A total number of 9 experimental runs and 3 central runs were designed considering two independent factors, namely, the concentration of modified BPNCC (%), and compression force (N). Every factor was considered at three levels of which the actual values are given in table 4.5. Disintegration time and % cumulative release were selected as responses, i.e., measurable dependent variables. Tablets compressed with modified BPNCC were characterized as per DOE protocol.

4.2.4.2 Determination of Disintegration time

As mentioned earlier under section 3.2.5.1, the disintegration time was found to be 180-195 seconds. The observations of disintegration time recorded for designed 12 experimental runs are compiled in figure 29.

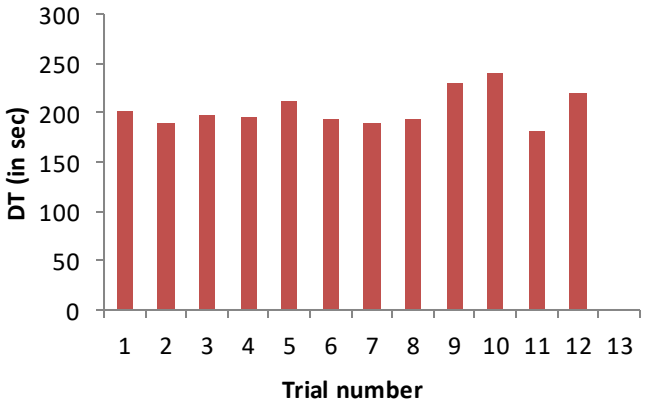

Figure 29 Disintegration time of DoE trial batches

4.2.4.3 Determination of % cumulative drug release

As mentioned earlier under section 3.2.5.2, % cumulative release of modified BPNCC experimental batch was found to be in the range of 78-89.9. Both the polynomial equations are given in table 24. Software-generated contour plots and 3D surface plots are shown in figure 30. The correlation of concentration of modified BPNCC and compression force to DT and % cumulative release was nonlinear.

Table 24 Summary of statistical analysis of responses using ANOVA

A. Calculated Statistical values:							
Sr. No.	Response	Reduced model	p-value	F-value	Lack of fit F-value	Correlation coefficient (R^2)	Adequate precision
1	Disintegration time	Quadratic	<0.0001	123.38	1.06	0.9788	33.9417
2	% cumulative release	Quadratic	<0.0001	152.93	0.4159	0.9829	33.1938
B. Polynomial equations:							
1	Disintegration time = +282.83 +127 A + 9 B + 42.67 A^2						
2	% cumulative release = +95.98 – 2.13 A – 2.65 B – 3.33 B^2						

To identify the optimized formulation, goals for responses were set as minimum disintegration time and maximum drug release. A numerical solution with the highest desirability, i.e., 1 was considered. The optimized formulation was suggested to contain 4.1% of modified BPNCC concentration at the compression force 2 N. Optimized formulation showed 175.5 second disintegration and 99.9 % cumulative release. The corresponding results were compared with the goals for responses.

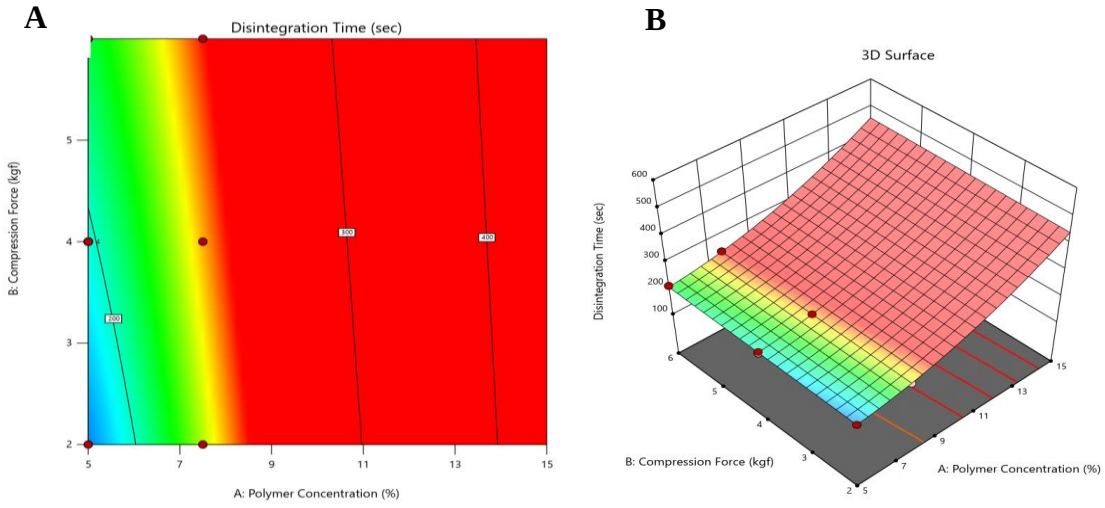

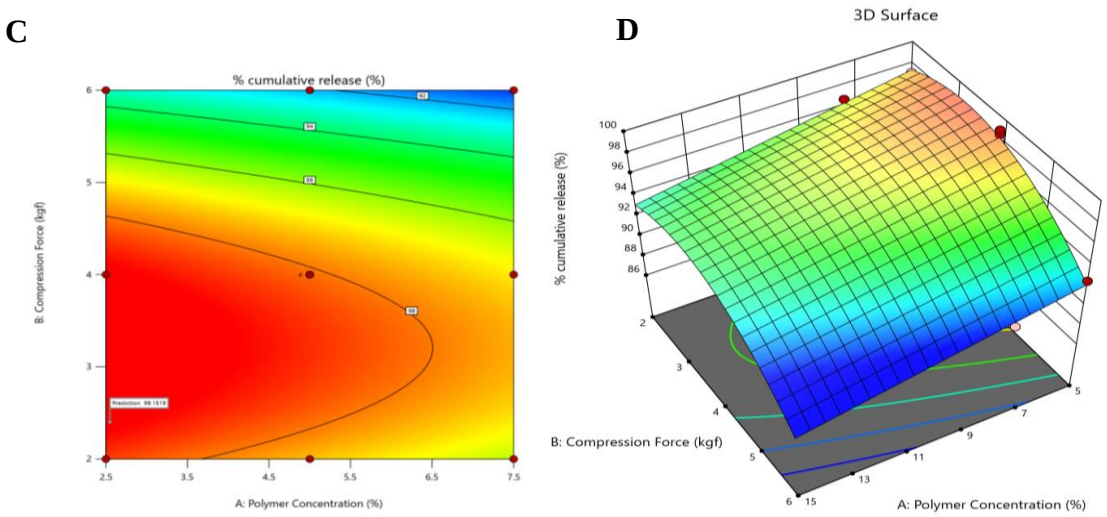

Figure 30 Contour (a,c) and 3D surface (b, d) plots demonstrating nonlinear correlation of factor A and factor B with both responses: (a-b) DT, (c-d) % cumulative release

4.2.5 COMPARISON OF DICLOFENAC POTASSIUM IR TABLETS PREPARED USING BPNCC, MODIFIED BPNCC, MARKETED MCC, GODAVARI MCC, AND MARKETED NCC

The tablets were compressed at 3 N using 3.5 % BPNCC concentration. Modified BPNCC was used at 2.5% concentration compressed at 2 N. All the tablets were evaluated for disintegration time and % cumulative release.

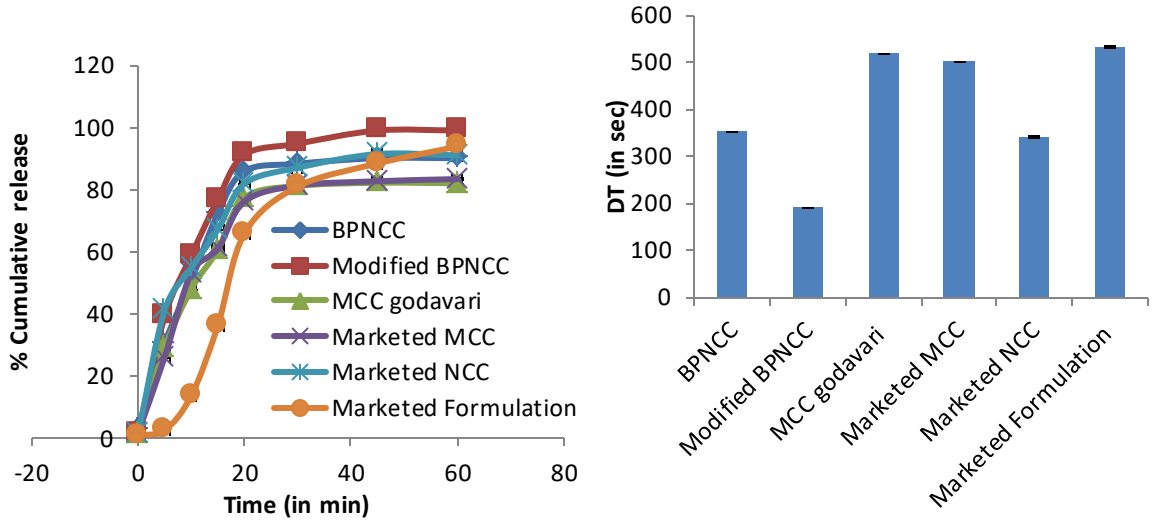

Figure 31 Comparison of in-vitro dissolution study and DT of Diclofenac potassium tablets prepared with different disintegrants

Modified BPNCC showed 99.03% drug release which is the highest among all the formulations. BPNCC and marketed BPNCC showed 90% and 91%, respectively. This shows effectiveness of extracted BPNCC. The lowest DT was showed by modified BPNCC which is 190.8 seconds. BPNCC and marketed NCC showed DT of 351 seconds and 340 seconds, respectively.

4.2.6 COMPARISON OF IVERMECTIN IR TABLETS PREPARED USING BPNCC, MODIFIED BPNCC, MARKETED MCC, GODAVARI MCC, AND MARKETED NCC

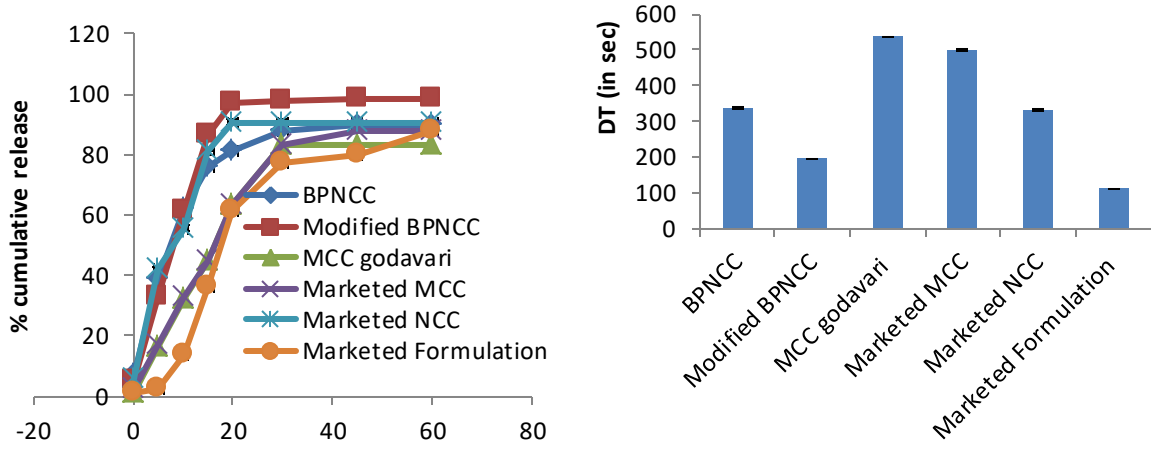

Figure 32 Comparison of in-vitro dissolution study and DT of Ivermectin tablets prepared with different disintegrants

Modified BPNCC showed highest 98.5% drug release and lowest release found to be with MCC godavari as disintegrants 83%. BPNCC as disintegrant showed 90.1% drug release. The lowest DT was showed by modified BPNCC around 194 seconds and the highest was obtained with Godavari MCC which was 505 seconds. BPNCC and marketed NCC showed DT of 353 seconds and 342 seconds, respectively.

4.2.7 COMPARISON OF TICAGRELOR IR TABLETS PREPARED USING BPNCC, MODIFIED BPNCC, MARKETED MCC, GODAVARI MCC, AND MARKETED NCC

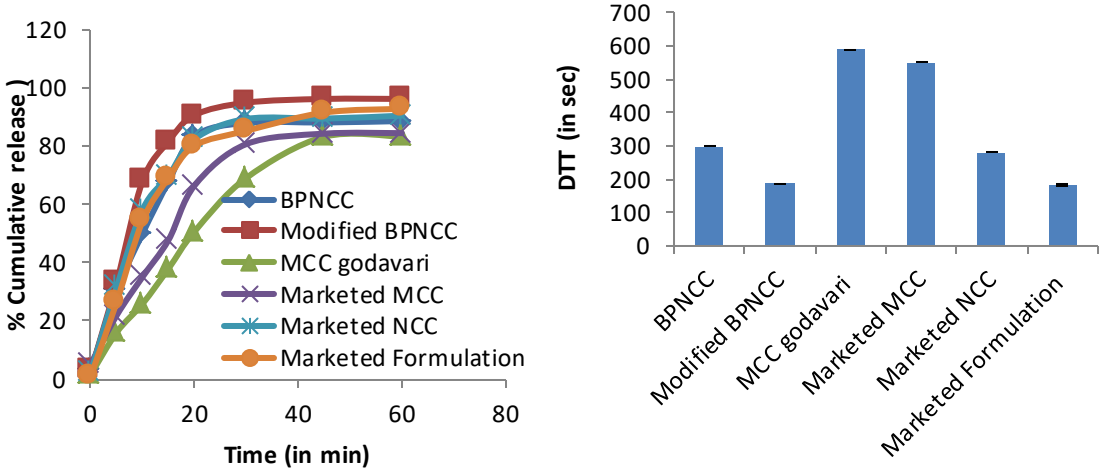

Figure 33 Comparison of in- vitro dissolution study and DT of Ticagrelor tablets prepared with different disintegrants

Modified BPNCC showed 96% drug release which is highest among all formulations. BPNCC showed 88.5% of drug release which is almost equal to the release of marketed NCC which is 90%. The disintegration time for all the tablets were compared and results showed the lowest DT was achieved in case of modified BPNCC which is around 187.8 seconds and the highest was obtained with godavari MCC which was 588.5 seconds. BPNCC showed DT 298 seconds which is similar to the DT of marketed NCC which is 281 seconds. BPNCC and modified BPNCC both showed disintegrating property.

4.2.8 COMPARISON OF RITONAVIR IR TABLETS PREPARED USING BPNCC, MODIFIED BPNCC, MARKETED MCC, GODAVARI MCC, AND MARKETED NCC

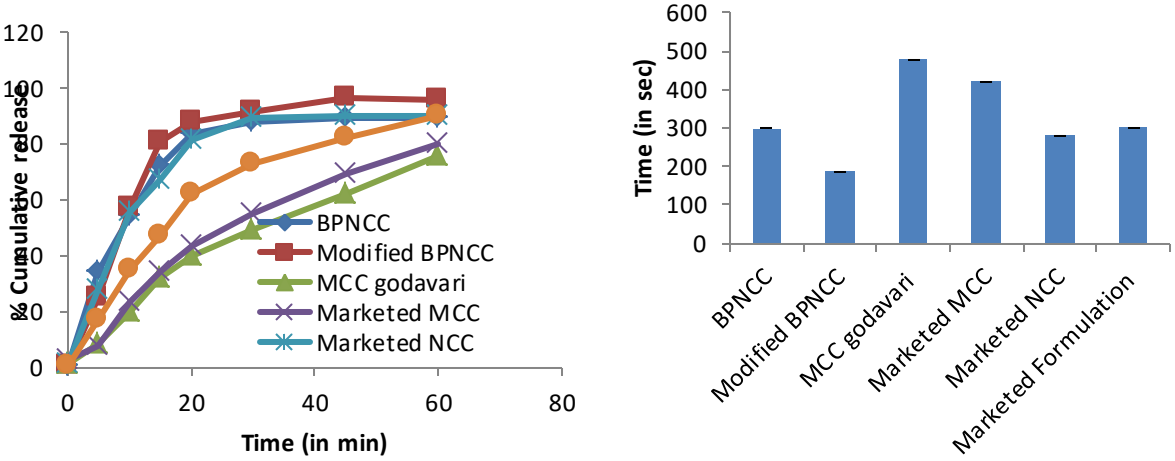

Figure 34 Comparison of in-vitro dissolution study and DT of Ritonavir tablets prepared with different disintegrants

Modified BPNCC showed 96 % drug release which is highest among all the formulations and lowest release was found to be with MCC godavari as disintegrants 75.3%. BPNCC showed 89.5% drug release which is equivalent to the marketed NCC which showed 90% drug release. As shown in figure 34, modified BPNCC showed the lowest DT which is 187 seconds. The highest DT was obtained with godavari MCC which was 478.5 seconds. BPNCC and marketed BPNCC showed DT of 298 and 281 seconds, respectively.

5 CONCLUSIONS

BPP and SCBMCC were used for the extraction of BPNCC and SCBNCC. Both the NCC was prepared by classic acid hydrolysis technique. SCBNCC was prepared using acid hydrolysis condition (55% H_2SO_4 concentration for 90 min at 55°C) and characterized further. SCBNCC showed needle shaped crystals having particle size of 145.3 nm and zeta potential was -29.7 mV, yield was found to be 35.5%, crystallinity increased 64% from 52%, and thermal analysis showed SCBNCC are stable. BPNCC was prepared using by optimizing the preparation condition. Optimized BPNCC showed crystallinity 62.18%, sharp needle kind of crystals was seen in SEM and TEM images confirming the shape of BPNCC. ATR-FTIR demonstrated complete removal of hemicellulose and lignin. The extracted SCBNCC and BPNCC worked as disintegrants. The disintegration time and dissolution study supported the hypothesis regarding solubility enhancers. They could be used as an alternative for various kinds of synthetic disintegrants. All the tablets were compared for Dissolution and DT. It was found that SCBNCC and BPNCC very well worked as a disintegrants showing disintegration time around 320-360 seconds for both. The release was found to be more than 80 % within 20 minutes. As proposed in the thesis, NCC would work as a super disintegrating agent. NCC alone did not work as a super disintegrating agent, but it worked well as a disintegrating agent. NCC modification was primarily done for solubility enhancement purposes. Primary amine helped increase the solubility of BCS class II and IV drugs (diclofenac potassium, Ivermectin, Ticagrelor and Ritonavir). Modified SCBNCC and modified BPNCC showed more than 90 % of drug release and DT in between 180-195 seconds. Overall, current work demonstrates the feasibility of newly synthesized excipients SCBNCC and BPNCC to be used as a competent disintegrant in less than 5% wt/wt. Modified SCBNCC and modified BPNCC also showed the good results for the category of super disintegrating agents.

6 REFERENCES

[1] Y. Habibi, L. A. Lucia, and O. J. Rojas, "Cellulose nanocrystals: Chemistry, self-assembly, and applications," *Chemical Reviews*, vol. 110, no. 6, pp. 3479–3500, Jun. 2010.

[2] S. Agate, M. Joyce, L. Lucia, and L. Pal, "Cellulose and nanocellulose-based flexible-hybrid printed electronics and conductive composites – A review," *Carbohydrate Polymers*, vol. 198, no. May, pp. 249–260, 2018.

[3] J. Sethi, M. Farooq, M. Österberg, M. Illikainen, and J. A. Sirviö, "Stereoselectively water resistant hybrid nanopapers prepared by cellulose nanofibers and water-based polyurethane," *Carbohydrate polymers*, vol. 199, pp. 286–293, Nov. 2018.

[4] X. Wu, J. Zhou, J. Huang, X. Wu, J. Zhou, and J. Huang, "Review 1800084 (1 of 10) Integration of Biomaterials into Sensors Based on Organic Thin-Film Transistors," 2018.

[5] T. Zhang, L. Yang, X. Yan, and X. Ding, "Recent Advances of Cellulose-Based Materials and Their Promising Application in Sodium-Ion Batteries and Capacitors," *Small*, vol. 14, no. 47, Nov. 2018.

[6] Q. Sun, B. Qian, K. Uto, J. Chen, X. Liu, and T. Minari, "Functional biomaterials towards flexible electronics and sensors," *Biosensors and Bioelectronics*, vol. 119, pp. 237–251, Nov. 2018.

[7] D. L. Aguilar *et al.*, "Scale-up and evaluation of hydrothermal pretreatment in isothermal and non-isothermal regimen for bioethanol production using agave bagasse," *Bioresource Technology*, vol. 263, pp. 112–119, 2018.

[8] M. Bolivar-Telleria *et al.*, "Second-Generation Bioethanol from Coconut Husk," *BioMed Research International*, vol. 2018, 2018.

[9] J. Qiu *et al.*, "Bioethanol production from wheat straw by phosphoric acid plus hydrogen peroxide (PHP) pretreatment via simultaneous saccharification and fermentation (SSF) at high solid loadings," *Bioresource Technology*, vol. 268, pp. 355–362, Nov. 2018.

[10] F. Delbecq and C. Len, "Recent Advances in the Microwave-Assisted Production of Hydroxymethylfurfural by Hydrolysis of Cellulose Derivatives-A Review," *Molecules (Basel, Switzerland)*, vol. 23, no. 8, 2018.

[11] M. Ehsanipour, A. V. Suko, and R. Bura, "Fermentation of lignocellulosic sugars to acetic acid by Moorella thermoacetica," *Journal of Industrial Microbiology and Biotechnology*, vol. 43, no. 6, pp. 807–816, Jun. 2016.

[12] L. Zhang, G. Xi, J. Zhang, H. Yu, and X. Wang, "Efficient catalytic system for the direct transformation of lignocellulosic biomass to furfural and 5-hydroxymethylfurfural," *Bioresource Technology*, vol. 224, pp. 656–661, Jan. 2017.

[13] F. Fu *et al.*, "Three-dimensional cellulose based silver-functionalized ZnO nanocomposite with controlled geometry: Synthesis, characterization and properties," *Journal of colloid and interface science*, vol. 530, pp. 433–443, Nov. 2018.

[14] S. M. F. Kabir, P. P. Sikdar, B. Haque, M. A. R. Bhuiyan, A. Ali, and M. N. Islam, "Cellulose-based hydrogel materials: chemistry, properties and their prospective applications," *Progress in biomaterials*, vol. 7, no. 3, pp. 153–174, Sep. 2018.

[15] L.-Y. Meng, B. Wang, M.-G. Ma, and J.-F. Zhu, "Cellulose-based Nanocarriers as Platforms for Cancer Therapy," *Current pharmaceutical design*, vol. 23, no. 35, Nov. 2017.

[16] J. Teng *et al.*, "Ultra-high mechanical properties of porous composites based on regenerated cellulose and cross-linked poly(ethylene glycol)," *Carbohydrate Polymers*, vol. 179, pp. 244–251, Jan. 2018.

[17] H. Ullah, F. Wahid, H. A. Santos, and T. Khan, "Advances in biomedical and pharmaceutical applications of functional bacterial cellulose-based nanocomposites," *Carbohydrate Polymers*, vol. 150, pp. 330–352, Oct. 2016.

[18] A. Arevalo-Gallegos, Z. Ahmad, M. Asgher, R. Parra-Saldivar, and H. M. N. Iqbal, "Lignocellulose: A sustainable material to produce value-added products with a zero waste approach—A review," *International Journal of Biological Macromolecules*, vol. 99, pp. 308–318, 2017.

[19] M. Kaur, M. Kumar, S. Sachdeva, and S. K. Puri, "Aquatic weeds as the next

generation feedstock for sustainable bioenergy production," *Bioresource technology*, vol. 251, pp. 390–402, Mar. 2018.

[20] C. Hutterer, G. Kliba, M. Punz, K. Fackler, and A. Potthast, "Enzymatic pulp upgrade for producing high-value cellulose out of a Kraft paper pulp," *Enzyme and Microbial Technology*, vol. 102, pp. 67–73, Jul. 2017.

[21] L. Kasirajan, N. V Hoang, A. Furtado, F. C. Botha, and R. J. Henry, "Transcriptome analysis highlights key differentially expressed genes involved in cellulose and lignin biosynthesis of sugarcane genotypes varying in fiber content OPEN."

[22] M. Mazarei *et al.*, "Functional Analysis of Cellulose Synthase CesA4 and CesA6 Genes in Switchgrass (Panicum virgatum) by Overexpression and RNAi-Mediated Gene Silencing," *Frontiers in plant science*, vol. 9, Aug. 2018.

[23] X. Yang, F. Berthold, and L. A. Berglund, "Preserving Cellulose Structure: Delignified Wood Fibers for Paper Structures of High Strength and Transparency," 2018.

[24] Z. Jiang, P. Zhao, and C. Hu, "Controlling the cleavage of the inter- and intra-molecular linkages in lignocellulosic biomass for further biorefining: A review," *Bioresource Technology*, vol. 256, pp. 466–477, May 2018.

[25] M. Kostag, K. Jedvert, C. Achtel, T. Heinze, and O. A. El Seoud, "Recent Advances in Solvents for the Dissolution, Shaping and Derivatization of Cellulose: Quaternary Ammonium Electrolytes and their Solutions in Water and Molecular Solvents," *Molecules 2018, Vol. 23, Page 511*, vol. 23, no. 3, p. 511, Feb. 2018.

[26] Y. Li, J. Wang, X. Liu, and S. Zhang, "Towards a molecular understanding of cellulose dissolution in ionic liquids: anion/cation effect, synergistic mechanism and physicochemical aspects," 2018.

[27] R. Liu, H. Yu, and Y. Huang, "Structure and morphology of cellulose in wheat straw," *Cellulose*, vol. 12, no. 1, pp. 25–34, 2005.

[28] N. Lin and A. Dufresne, "Nanocellulose in biomedicine: Current status and future prospect," *European Polymer Journal*, vol. 59, no. July, pp. 302–325, 2014.

7 RESEARCH OUTCOMES

Publications from PhD

Sr. No	Details	Journal (IF)	Status
1.	A Disintegrant from waste source: NCC extracted from Sugarcane Bagasse-Derived Microcrystalline Cellulose	Drug delivery (6.8)	Under review
2.	Application of Quality by Design Approach to Investigate the Effect of Nano Crystalline Cellulose Extracted from Agricultural Waste as a Disintegrant	Chemical papers (2.1)	Revision submitted
3.	**Banana Peel Waste: An Emerging Cellulosic Material to Extract Nanocrystalline Cellulose**	**ACS Omega (4.12)**	**Published**
4.	**Biomass and waste materials as potential sources of nanocrystalline cellulose: Comparative review of preparation method (2016 till date)**	**Carbohydrate Polymer (7.18)**	**Published**

Publications other than PhD

Sr. No	Details	Impact factor	Status
1.	**Organ-On-A-Chip Technology: An In-depth Review of Recent Advancements and Future of Whole Body-on-chip** **Risabh Driver, Shweta Mishra***	**Biochip Journal (4.2)**	**Published**

Book Chapters

Sr. No	Authors	Title of Book	Title of the chapter	Publisher
1	**Shweta Mishra**, Anil M. Pethe	Nanotechnology in wood Pharmaceutical applications and pulp engineering (Elsevier)	**Pharmaceutical applications of Nanocellulose**	Elsevier

PRESENTATIONS:

1. **Shweta Mishra**, Anil M. Pethe. Use of Stents in Coronary Heart Disease. ***50th Annual Conference of Indian Pharmacological Society (IPSCON-2017).*** Organized by Shobhaben Pratapbhai Patel School of Pharmacy & Technology Management, SVKM's NMIMS, Mumbai & Indian Pharmacological Society. 15-17th February, 2018
2. **Shweta Mishra**, Bala Prabhakar, "A Disintegrants extracted from banana peel waste". AAPS Northeast regional discussion group organized by St. John's University, Queens, New york. 31st march 2023

Ms. Shweta Mishra
Ph.D. Student

Dr. Bala Prabhakar
Research Supervisor